Asymptotic analysis of multi-layered waveguides with contrast parameters

Mohammed Omar S Alkinidri

Submitted in partial fulfilment of the requirements of the degree of
Doctor of Philosophy

Keele University
School of Computing and Mathematics

June 2021

I certify that this thesis submitted for the degree of Doctor of Philosophy is the result of my own research, except where otherwise acknowledged, and that this thesis has not been submitted for a higher degree to any other university or institution.

Mohammed Alkinidri

June 2021

Acknowledgements

Undertaking this PhD has been a truly life-changing experience for me and it would not have been possible to do without the support and guidance that I received from many people. My dream to succeed in my PhD journey would not have been achievable if I do not receive great support from King Abdulaziz University, which provided me with full scholarship to do the PhD at Keele University. This has been one of the greatest opportunities in my life. I am indebted to them. No scientific progress is possible without standing on the shoulders of giants, and it was my good fortune to have Prof. Julius Kaplunov and Dr. Ludmila Prikazchikova as supervisors. I am greatly indebted to them for their inspiring, enthusiastic supervision, willingness to help and devoting so much of their valuable time during the time of preparing this thesis. They were available with useful advice, encouragement and very valuable discussion. It goes almost without saying that this particular thesis could not have been written without them. Moreover, they encouraged me to participate in many conferences from which I benefited a lot. Their constructive criticism on my research made me mature as a mathematician and for that, I am most grateful. Finally, but by no means least, thanks go to my mother "Aisha", my father "Omar "(May Allah have mercy on him), my wife " Bayan", my daughter " Rittal" and my siblings for almost unbelievable support throughout this challenging yet rewarding journey. They are the most important people in my world and I dedicate this thesis to them.

Abstract

The research is investigating anti-plane shear of a strongly inhomogeneous dynamic asymmetric laminate. Two types of contrast are considered, including those for composite structures with thick or thin stiff outer layers. In all types of contrast, the value of the cut-off frequency corresponding to the lowest harmonic tends to zero. For two modes, i.e. the fundamental mode and aforementioned lowest harmonic, the shortened dispersion relations and the associated formulae for displacement and stresses are obtained. As a particular case a symmetric three-layered plate is studied. The asymptotic equations of motion are derived with the evaluation of the validity range for each of two considered setups of contrast parameters. In addition, the asymptotically justified boundary conditions are derived by the generalisation of the Saint Venant's principle to high-contrast structures.

Contents

List of Figures

List of Tables

Chapter 1

Introduction

1.1 State of the Art

Layered elastic structures have numerous industrial applications. For example, such structures are used within a great number of civil and mechanical engineering projects and also in aircraft and automotive design along with several areas in geo- and bio-mechanics. They are also of interest for high-tech domains including meta-material technology.

Sandwich structure is seemingly the most popular example of a laminate. They consist of relatively thin and stiff outer layers divided by a thick and soft lightweight core. Among the materials used for outer layers there are wood, metal sheets, while the core is often composed of various polymers, including those in the form of honeycombs. The sandwich panels are utilised in various engineering constructions, having simultaneously numerous advantages such as high stiffness and light weight, see for example Zenkert [1995].

Thus, sandwich composites are extensively exploited in modern engineering design, aiming at weight reduction, e.g. see Vinson [1999]. They are used not only in the aerospace industry where sandwiches have been initially implemented, see Dutton et al. [2004], but also in trains, racing cars and high-speed marine crafts, see Arbaoui et al. [2015]. In particular, for high speed trains a composite sandwich structure is examined in Zinno et al. [2010] and Kim and Chung [2007]. We also mention Torre and Kenny [2000] concerned with composite sandwich panels as structural components of trains and buses.

In contrast to conventional sandwich structures layered composites may also possess soft skins and stiff inner layers. A precipitator plate is a good example of this type of laminates. It is an important part of gas filters for collecting dust particles from gas streams e.g. see Tassicker [1972] and Lee and Chang [1979].

Ultra-light photovoltaic layered structures are used in solar cars and satellite solar panels, e.g. see Renno [2008], studying solar aircraft. This is a multi functional low cost concept enabling weight reduction and energy saving, see also Mines et al. [1998], Rion [2008], and Beral [2007].

Laminated glass plates and beams are another example of thin structures exhibiting high contrast in material and geometrical properties. Laminated glass which is widely used in automotive and civil engineering are usually composed of three layers. Among them there are two relatively thick claddings and a soft slim polymeric core. This layout enables to achieve high stiffness along with other important technical properties, e.g. see Aşık and Tezcan [2005].

Layered composites also find applications in the fast developing area of meta-materials. These materials demonstrate unique properties originating from periodically arranged layers having high contrasting parameters, e.g. see Martin et al. [2012].

Multi-layered structures have been of particular interest for theoretical analysis since long ago. In particular, main focuses are in mathematics and mechanics of solids. There are numerous publications on the subject and it is hardly possible to present a complete account of all the developments in this area. In what follows we concentrate only on most influential deliveries e.g. substantial books by Reddy [2003] and

Mikhasev and Altenbvach [2019] as well as on the output closely related to the main theme of the thesis.

Mechanics of sandwich plates has a remarkable history. Apparently, the first analytical investigation of bending and buckling of sandwich plate structures was proposed by Reissner [1947]. In this study, the author considered a sandwich plate with relatively stiff outer layers. In this case, in addition, the thickness of the outer layers is assumed to be much smaller than that of the core layer. A simple solution based on ad-hoc hypothesis on the sandwich behaviour is obtained.

Similar analysis was also conducted by Hoff [1950], who used a variational approach for deriving the differential equations and boundary conditions governing sandwich plates. In another study, Eringen [1951] found the solution of the partial differential equations modelling bending and buckling of rectangular shaped sandwich plates. The core of the rectangular plate is supposed to be isotropic. The main focus of the above mentioned papers is elastic buckling. Also, Cheng [1961] investigated the Reissner equation, see Reissner [1947], and also initiated investigation of the connection between Reissner and classical plate theories. In this paper the expressions for moment, shear and deflection are also provided. We also mention two substantial general reference work reporting on numerical modelling of sandwich structures, see Ha [1990] and Noor et al. [1996].

Analysis of waves in layered infinite media, mainly inspired by needs in seismology, logically precedes dynamic treatment of elastic thin wave-guides in the shape of elastic plates, shells and beams. The classical example includes the famous paper Ewing et al. [1957], see also Abramovici and Alterman [1965] reporting on further numerical results for a layered half space.

Structural dynamics can be understood with the help of examination of associated dispersion relations. Analysis of the dispersion relations for homogeneous layers was the subject of many publications, beginning with Lamb [1917]. We also mention later substantial contributions Tolstoy and Usdin [1957], Mindlin [1960] along with the books Kaplunov et al. [1998] and Achenbach [2012]. Another popular shape corresponds to a cylindrical shell, see Beresin et al. [1995].

Elastic wave propagation in isotropic sandwich plates with the emphasis on the flexural wave propagation is analysed in Mindlin [1959] and Yu [1960]. Later on, both numerical and asymptotic techniques were adapted. In particular, Jones [1970] computed the dispersion curves for quasi-flexural and quasi-extensional waves. The flexural wave approximation appears to be in accordance with the classical plate theory at a moderate wavelength range. On the other hand, extensional vibrations correspond to the long wavelength limit. The results for two, three, four and five-ply laminates are given by Kulkarni and Pagano [1972]. The solution to the plane-strain problem

with the continuity conditions of traction and displacements along the interfaces is presented in Lee and Chang [1979]. They consider both flexural and SH-waves. The numerical solutions of the obtained dispersion relations are derived.

Waves propagation in symmetric three-layered fibre-reinforced elastic structures is considered by Baylis and Green [1986a,b]. Numerical data is obtained for two specific directions of wave propagation. The results of parametric analysis for various ratios of core thickness to outer layer thickness are also included.

Comparisons of the solutions in classical structural theories and those coming from shear deformation formulations are presented in particular in Wang and Wang [2016] and Qatu [2004]. The cited textbook Wang and Wang [2016] considers linear free vibrations of composite structures of canonical shapes including thick ones. Approximate theories for laminated composite structures along with finite element models can be found in Renno [2008]. In addition, we mention a useful review Kreja [2011] dealing with the computational modelling of laminates.

The paper Naumenko and Eremeyev [2014] starts from the approximations to the exact Rayleigh-Lamb dispersion relation. As a result a comprehensive Timoshenko-Reissner type model is found to be robust for treating thin laminated plates. The results are applied to modelling of laminated glass and photovoltaic panels.

The first order shear deformation plate theory was also applied for analysis of laminates with thin and soft core layers in Nguyen et al. [2008]. The results of this paper are useful for computation of laminated glasses and photovoltaic panels.

Basic asymptotic analysis found to be valuable for interpretations of dispersion relations. For a long time its range was restricted to low-frequency vibrations. The qualitative study of the dispersion relation over the high-frequency range starts from several papers cited in the general reference work Ainola and Nigul [1965] and Grigolyuk and Selezov [1973]. Among later publications, taking into consideration pre-stressed and layered structures we mention Kaplunov et al. [2000b], Pichugin and Rogerson [2002a], Kaplunov et al. [2002a], Leungvichcharoen and Wijeyewickrema [2003], Lashhab et al. [2015], Nolde et al. [2004], Rogerson et al. [2007]. In particular, the investigation of small amplitude vibrations in a symmetric, incompressible, pre-stressed three-layered plate is developed in Rogerson and Sandiford [1996] and Rogerson and Sandiford [1997]. In these papers numerical and analytical results were obtained for both short and long wave limits. The effect of imperfect bonding have been also investigated numerically in the first of the cited papers. In the second one this effect was further treated analytically at high and low wave number limits in the case of antisymmetric motion. The cut-off frequencies for harmonics are also studied.

The highly original paper Chapman [2013] also deals with long-wave low-frequency

analysis of dispersion relation for a multi-layered plate. For the first time it develops finite product approximation adapted for steady state problems in elastic wave propagation. Anti-symmetric waves in a three-layered elastic plate are given a special attention. The obtained results are compared with two well known approximations, including Tiersten's thin-skin formulation and the Timoshenko theory.

Dispersion of elastic waves for the unbounded three-layered isotropic sandwich plate under heavy fluid loading is analyzed in Sorokin [2004]. However, alternatives to the full 3D hydro-elasticity are also studied. In particular, it is demonstrated that simplified structural theories give pretty accurate estimations over certain parameter ranges.

Among all the variety of vibration modes, the fundamental one originating from zero frequency is usually of particular interest for various practical needs. This mode involves the most important from the technical viewpoint long wave low frequency range. However, according to the studies of Kaplunov and Markushevich [1993], Kaplunov et al. [2002a], and many others Berdichevskii [1977], Tovstik [1992], the long-wave behaviour of harmonics may be also very relevant in case of more advanced applications, including in particular modelling of resonators and other acoustic devices.

The asymptotic methodology is very powerful in dynamics of thin elastic structures, e.g. see the monographs Goldenveizer [1976], Kaplunov et al. [1998], Berdichevsky [2009], Aghalovyan [2015], Le [2012]. It plays a central role in the considerations within the thesis and is reviewed in the next section. Here, as an example we only mention the paper by Lutianov and Rogerson [2010], analysing long-wave motions in three-layered isotropic plate and deriving the associated 2D asymptotic models. It is noted that the asymptotic governing equations for a three-layered plate are similar to those for a single layer in case of both low- and high-frequency motions.

The asymptotic methodology has been more recently adapted for structures with high contrast properties, see Berdichevsky [2010], Tovstik and Tovstik [2017], Boutin and Viverge [2016], Kaplunov et al. [2017a,b], Prikazchikova et al. [2020] and Lee and Chang [1979], Horgan [1998], Ryazantseva and Antonov [2012], Viverge et al. [2016], Boutin and Viverge [2016], Berdichevsky [2010], Liu and Bhattacharya [2009], Tovstik and Tovstik [2017]. In particular, in Kaplunov et al. [2017a] multi-parametric analysis of a three-layered symmetric plate was developed taking into account the effect of small-large ratios of thickness, densities and stiffness of the layers. The condition on the aforementioned ratios are derived ensuring the smallest shear cut-off to be asymptotically close to zero, see Kaplunov et al. [2016, 2019b]. In this case the Kirchhoff plate theory is valid over a rather restricted domain. This motivates

deriving of two-mode approximations which contains both the fundamental bending mode and lowest shear harmonic. There are some setups of contrasting problem parameters resulting in non-uniform asymptotic behaviour, e.g. see Kaplunov et al. [2017a] considering a plane problem for a symmetric sandwich plate. In this case, the associated asymptotic behaviour appears to be composite, i.e. it is valid only over narrow non-intersecting vicinities of zero and lowest cut-off frequencies.

It is worth noting that the cut-off frequencies of three-layered plate correspond to the eigen frequencies of three-component elastic rod, e.g. see Kaplunov et al. [2016] and Kaplunov et al. [2019b] dealing with multi-component structures.

Further insight into multi-parametric behaviour, investigated within the plane-strain framework in Kaplunov et al. [2017a], has been developed for its less technical anti-plane counterpart in Prikazchikova et al. [2020] concerned with the antisymmetric vibration of a three-layered plate. This formulation does not assume a fundamental mode. In this case wave propagation takes place above the lowest cut-off with an asymptotically small value. In addition to polynomial approximations to full dispersion equations, the partial differential equations corresponding to the long-wave low-frequency limit were presented.

We specially remark on the paper Liu and Bhattacharya [2009] dealing with elastic wave propagation in a sandwich composed of two stiff face-plates and a heavy compliant core. In this paper the wave equations are transformed to a Hamiltonian system tackled by the transfer matrix technique. The long-wave limit is studied in great detail, including the fundamental vibration mode.

Another recent important paper by Tovstik and Tovstik [2017] considers highly heterogeneous material, including laminates. The cases in which neither Kirchhoff-Love nor Timoshenko - Reissner theories are applicable are highlighted.

1.2   Asymptotic methods for thin elastic structures

The asymptotic derivation of 2D static equations for thin plates and shells starting from 3D equilibrium equations in linear elasticity originated from pioneering contributions by Friedrichs and Dressler [1961], Goldenveizer [1966, 1980], Reiss and Locke [1961], Reissner [1963] and Aksentian and Vorovich [1963].

Similar approach can be adapted to low-frequency dynamics, e.g. see Goldenveizer et al. [1993] and references therein along with more recent papers by Pichugin and Rogerson [2002a] and Kaplunov et al. [2000b] that focus on pre-stressed plates.

Asymptotic methods can be also implemented over the high-frequency domain, including both short-wave and long-wave limits. In this case, the high frequency approximation in contrast to more conventional low-frequency one demonstrates sinusoidal variation across the thickness of the structure, see Kaplunov et al. [1998]. For short wave approximations a typical wavelength is of thickness order, while for long-wave approximations it is greater than the thickness. The general classification for the asymptotic approximation in dynamic structures is presented in Kaplunov et al. [1998], see also Beresin et al. [1995].

In various setups this includes anisotropic structures (Kaplunov et al. [2000a]), pre-stressed structures (Pichugin and Rogerson [2001, 2002b], Kaplunov et al. [2000b]), high-frequency long-wave modes (Kaplunov et al. [2005], Gridin et al. [2005]), fluid structure interaction (Kaplunov and Markushevich [1993]), layered structures (Lutianov and Rogerson [2010], Ryazantseva and Antonov [2012], Craster et al. [2014], Lashhab et al. [2015], Nolde et al. [2004] and structures with non-classical boundary conditions along faces (Kaplunov et al. [2000a], Kaplunov and Nolde [2002], Rogerson et al. [2007], Nolde and Rogerson [2002]). As an example of high-frequency short-wave analysis we again mention Kaplunov et al. [1998] along with the generalisation to a pre-stressed plate reported in Kaplunov et al. [2002b] as well as Rogerson et al. [2004] treating a longitudinally inhomogeneous cylindrical shell.

For example, Pichugin and Rogerson [2002a] implement the asymptotic technique for examining flexural plate motion near the cutoff frequencies of a pre-stressed incompressible elastic plate. Acoustic radiation and forced thickness vibrations in a fluid loaded elastic layer is studied in Kaplunov and Markushevich [1993]. The consideration in the cited paper starts from 1D equation of motion governing long-wave high-frequency vibration taking into account radiation into the fluid. 2D equations of motion are derived in the paper by Kaplunov et al. [2002a] dealing with high-frequency long-wave vibrations of a thin elastic shell with clamped faces. Similar asymptotic approach is applied for analysis of high-frequency long-wave trapped modes in the paper by Kaplunov et al. [2005], analysing linear isotropic elastic plates and rods.

Asymptotic analysis of initial and boundary conditions is particularly sophisticated and important. It is remarkable, that the majority of the publication on the subject are focused on the derivation of the differential equations of motion, overlooking the impact of initial and boundary conditions. Asymptotic treatment of the boundary conditions usually starts from the properly adapted Saint-Venants principle expressing a rapid decay of self-equilibrated edge data, e.g. see Goldenveizer [1976, 1998], Gregory and Wan [1984] and Gregory and Wan [1985]. The decay conditions for a semi-infinite elastic strip play a key role in the implementation of the Saint-Venant's

principle. Initially established for statics, see Gregory and Wan [1984] and Gusein-Zade [1965], these conditions later on were extended to dynamics Babenkova and Kaplunov [2004, 2005].

Superposition of high-frequency long-wave approximations along with more classical low-frequency long-wave ones has to be investigated in order to establish the initial conditions in 2D plate theories, see Kaplunov et al. [2006] and Nolde [2007]. Publications by Goldenveizer et al. [1993], Popescu and Hodges [2000], Nolde et al. [2018], Stephen [1981, 2006], Berdichevskii [1979], Berdichevskii and Starosel'skii [1983], Le [2012] and Elishakoff et al. [2015] are aimed at higher order low-frequency analysis applied to justification and refinement of ad-hoc Timoshenko-Reissner structural theories.

We also mention the concept of composite expansions assuming asymptotic behaviour only at distinct limiting cases without an emphasis on less important intermediate regions, e.g. see Van Dyke [1975] and Andrianov et al. [2013]. Recently, composite wave models have been constructed for thin and periodic structures in Erbaş et al. [2018b, 2019] and Colquitt et al. [2019].

Finally, we mention a series of fresh contributions concerned with long-wave asymptotic analysis in statics and dynamics of elastic coatings Aghalovyan [2015], Dai

et al. [2010], Kaplunov et al. [2018, 2019c], Chebakov et al. [2016]. These publications study thin structures modelling elastic coatings and result in the derivation of effective boundary conditions or elastic foundation models, see also Kudish et al. [2020, 2021]. Here we reiterate that the original problem in mechanics of thin-walled bodies is formulated for traction free (or loaded) faces, but not for clamped ones, see Erbaş et al. [2018a]. In the latter case, also corresponding to contact problems, low-frequency extensional modes can only be observed for a sliding contact. Other types of low-frequency modes appear only over the high-frequency domain.

1.3 Objectives and outline of the thesis

The thesis deals with low-frequency long-wave vibrations of elastic layered plates composed of the layers with distinct geometric and material properties. The main inspiration for the developed research is due to the possibility of extra low-frequency shear modes and asymptotic analysis of the associated dynamic phenomena, including two-mode low-frequency behaviour of strongly inhomogeneous laminates. The thesis is aimed at elucidation of the effect of high contrast in problem parameters on the peculiarities of low-frequency long-wave motions.

In this work we insert asymmetry in the formulation of Prikazchikova et al. [2020], considering antiplane shear of a symmetric three-layered plate, resulting in a two-mode low-frequency behaviour. The low-frequency shear mode studied in the cited paper now interacts with the fundamental one, propagating with zero cut-off frequency. For a symmetric plate these two modes are separated from each other, making possible to analyse the low-frequency shear mode without the reference to the fundamental one.

The observed two-mode phenomena obviously occur only under certain limitations on the problem parameters; i.e. this happens only when the smallest cut-off tends to zero at the limit in which the ratios of stiffnesses, densities or thicknesses of the layers take small or large values.

In what follows, we deal with the two-mode long-wave low-frequency approximations of the full dispersion relation for shear waves, similarly to Kaplunov et al. [2017a], but for a simpler scalar problem. This is promising for the deeper insight in dynamics of high-contrast layered structures, including not only asymptotic considerations of the dispersion relation, but also the derivation of the associated equations of motions. The algebra in the thesis is obviously more involved than that in Prikazchikova et al. [2020], since the plate motion now cannot be split into symmetric and antisymmetric components.

The dissertation is organised as follows. The introductory Chapters 1 and 2 contain

a literature review and general relations in linear elasticity, respectively.

The Chapter 3 is concerned with the toy problem for a two-layered plate with mixed

boundary conditions along the faces and the conditions of a perfect contact along the

interface. The stiffness of the lower layer is assumed to be much greater than that of

the upper layer. The ratio of the densities of these layers is considered to be of the

same order. This type of contrast is adapted in all the forthcoming chapters apart

from Chapter 6. Both shortened dispersion relation and associated 1D equation of

motion are derived. They govern long-wave low-frequency antiplane shear vibrations

with the smallest shear cut-off frequency. As might be expected, the obtained results

are in agreement with the developments in Prikazchikova et al. [2020], dealing with

the low-frequency antisymmetric (with respect to the midplane) motion of a three-

layered plate with traction free faces.

In Chapter 4 we generalise the approach developed in Chapter 3, see also Kaplunov

et al. [2017a] and Prikazchikova et al. [2020] for antiplane shear of a three-layered

asymmetric laminate with traction free faces. We restrict ourselves to the high con-

trast scenario in which the outer layers are stiff, while the inner one is relatively

soft; in doing so, we start from the assumptions on the contrast parameters, adapted

in the previous chapter. The formulated scalar problem seems to be the simplest

example in structural mechanics supporting a two-mode long-wave low-frequency behaviour involving both the fundamental mode and lowest shear harmonic. In this chapter we derive and analyse the full transcendental dispersion relation only. It is shown that the leading order shortened polynomial equation can be factorised into two ones corresponding to the fundamental mode and the lowest shear harmonic. The latter equation also approximates a slow quasi-static (and static at zero frequency) decay below the smallest cut-off frequency, when the lowest shear harmonic is still evanescent. In spite of asymmetry of the problem, the factorisation of the shortened dispersion relation takes place due to a 'weak' coupling of two retained modes, supported by the considered high contrast. Numerical comparison of the full and two-mode shortened polynomial dispersion relations are presented.

The Chapter 5 is the central for the thesis. In this chapter we first use a preliminary insight originating from the asymptotic dispersion analysis in the previous chapter for deriving 1D equations of motion generalising the technique in Prikazchikova et al. [2020], see also earlier publications Goldenveizer et al. [1993], Kaplunov et al. [1998], oriented to single layer elastic structures. The derived fourth order 1D operator is also factorised into two second-order ones corresponding to the fundamental mode and the lowest shear harmonic. As above, the operator governing the harmonic describes a decay below the cut-off. In addition, by the long-term tradition for elastic plates

and shells, e.g. see Goldenveizer [2014], the obtained equations are also presented in terms of stress resultants, stress couples and also the average displacement and the angle of rotation.

Apparently for the first time in mechanics of layered structures, we implement the Saint-Venants principle, e.g. see Love [2013], combined with asymptotic considerations, taking into account high contrast, for extending the powerful procedures established for homogeneous plates and shells, e.g. see Goldenveizer [1976], Gregory and Wan [1984, 1985], Goldenveizer [1998]. We begin with the static decay conditions for a semi-infinite three-layered strip subject to homogeneous boundary conditions along the faces and prescribed anti-plane shear stresses at the edge, see for example Gregory and Wan [1984], Gusein-Zade [1965], Babenkova and Kaplunov [2004]. In contrast to the previous considerations, we expect a strong decay of the boundary layer, i.e. localisation of the stress field over a narrow edge vicinity. In this case slowly decaying solutions, characteristic of high-contrast laminates, e.g. see Horgan [1998], are not counted as boundary layers.

Two decay conditions are formulated in this chapter. The first of them is expresses the self-equilibrium of the prescribed shear stress in agreement with the classical Saint-Venants principle. The second one is of asymptotic nature and has no obvious counterparts within the non-contrast setup. This condition is compared with the

exact Laplace transform solution for a symmetric plate. The decay conditions immediately result in the sought for boundary conditions at the edge of a finite length three-layered plate, similarly to Babenkova and Kaplunov [2003] and many others.

In Chapter 6 we study another type of high contrast, for which the two stiff outer layers are assumed to be much thinner than a soft inner one. In addition, we consider a greater than before contrast in densities of the layers. We derive two-mode shortened approximations of the full dispersion relation, obtained in the Chapter 4. It is shown that in contrast to the consideration in that chapter, the derived two-mode approximation is not uniformly valid. It's range of validity consists of two non overlapping vicinities of zero and the smallest shear cut-off frequencies. As before, the asymptotic results are compared numerically with the exact ones. A clear gap within the validity range of the two-mode polynomial approximation is observed in the plotted graphs. The obtained scaling may be applied to the derivation of a 1D equation of motion corresponding to the parameter setup studied in this chapter.

In Chapter 7 the conclusions of the thesis are briefly summarised along with several suggestions for a possible follow-up programme.

The results of the thesis were partly published in the publications Alkinidri et al. [2019, 2020], Kaplunov et al. [2021], written in collaboration with the supervisory

team.

Chapter 2

Governing equations

The basic relations in continuum mechanics are briefly addressed. The constitutive relations in linear elasticity are written down. 2D equations of motion studied in what follows are presented.

2.1   Deformation, stress tensor and balance of lin-

ear momentum

Consider a continuum medium that undergoes deformation. Let $\mathbf{u}(x_1, x_2, x_3, t)$ be a

small displacement vector of a material point, where t represents time and u_1, u_2, u_3

are its Cartesian components. This vector can be written as

$$\mathbf{u} = u_i \mathbf{v}_i, \tag{2.1}$$

where $\mathbf{v}_i$, $i = 1, 2, 3$ are unit vectors along Cartesian axis and summation over re-

peated index is assumed. It is emphasised that the summation convention is only

assumed within this chapter and is not adopted throughout the remaining thesis. In

this case the symmetric second order infinitesimal strain tensor ε has the components,

e.g. see Spencer [1988]

$$\varepsilon_{ij} = \frac{1}{2} \left(\frac{\partial u_i}{\partial x_j} + \frac{\partial u_j}{\partial x_i} \right), \qquad i, j = 1, 2, 3. \tag{2.2}$$

We also consider the surface traction vector τ^n, which defines the force per unit area

across a surface with a unit outward normal n. The traction components τ_j^n serve to

define the stress tensor σ using the formula

$$\tau_i^n = \sigma_{ji} n_j. \tag{2.3}$$

Along with the above mentioned strain tensor, the latter tensor plays a fundamental role in a linear elastic model, adapted in this thesis.

Now consider an elastic body occupying a closed region D with the boundary T having an outward unit normal $\mathbf{n}$. Then the law of conservation of linear momentum is expressed in the form, e.g. see Spencer [1988]

$$\iint_T \tau_i^n dA + \iiint_D \rho b_i dV = \iiint_D \rho \frac{\partial^2 u_i}{\partial t^2} dV, \tag{2.4}$$

where b_j are the components of the body forces per unit mass acting on the particles in D, ρ is density of the elastic material and dA and dV denote area and volume differentials, respectively.

In the left hand side the surface integral can be transformed into a volume one using the divergence theorem, see Spencer [1988]. Substitution of (2.3) into (2.4) together

with aforementioned observation results in

$$\iiint_D \left(\frac{\partial \sigma_{ji}}{\partial x_j} + \rho b_i - \rho \frac{\partial^2 u_i}{\partial t^2} \right) dV = 0. \tag{2.5}$$

Since relation (2.5) must hold in any part D of the elastic body, we obtain the following equation

$$\frac{\partial \sigma_{ji}}{\partial x_j} + \rho b_i = \rho \frac{\partial^2 u_i}{\partial t^2}, \tag{2.6}$$

corresponding to the equation of motion in linear elastodynamics.

2.2   Stress and strain relations for homogeneous isotropic linearly elastic solid

The linear relations between the components of the stress and strain tensors can be sought as a natural generalisation of Hooke's law in the one-dimensional case. In the general case they can be written as

$$\sigma_{ij} = C_{ijkl} \varepsilon_{kl}, \tag{2.7}$$

where C_{ijkl} are the components of the fourth order elasticity tensor, satisfying the identities

$$C_{ijkl} = C_{jikl} = C_{klij} = C_{ijlk}. \tag{2.8}$$

The medium is called homogeneous if all the coefficients C_{ijkl} are constants. In case of elastic isotropy constants C_{ijkl} can be expressed as

$$C_{ijkl} = \lambda\delta_{ij}\delta_{kl} + \mu(\delta_{ik}\delta_{jl} + \delta_{il}\delta_{jk}), \tag{2.9}$$

where λ and μ are Lame elastic constants, e.g. see Achenbach [2012] and δ_{ij} is Kronecker delta with $\delta_{ij} = 0$ for $i \neq j$ and $\delta_{ij} = 1$ if $i = j$.

Expression (2.9) can be inserted into equation (2.7) leading to

$$\sigma_{ij} = \lambda\delta_{ij}\varepsilon_{kk} + 2\mu\varepsilon_{ij}. \tag{2.10}$$

The latter are usually referred to as the constitutive equations for an isotropic linear elastic solid.

2.3 Equations of Motion

2.3.1 1D motion

Consider first the components of the stress tensor depending only on one spatial variable x_1. Then the equations of motion reduce to

$$\frac{\partial \sigma_{1i}}{\partial x_1} + \rho b_i = \rho \frac{\partial^2 u_i}{\partial t^2}, \qquad i = 1, 2, 3. \tag{2.11}$$

In particular, for the longitudinal 1D motion we have $i = 1$ in the above equation.

2.3.2 2D motion

In case of two-dimensional problems, the components of stress tensor and forces of body are dependent on two variables, e.g. x_1 and x_2. Therefore, the equations of motion can be obtained from (2.6) by setting $\frac{\partial}{\partial x_3} = 0$. Thus, we can separate the system of equations (2.6) into two uncoupled systems as:

$$\frac{\partial \sigma_{31}}{\partial x_1} + \frac{\partial \sigma_{32}}{\partial x_2} + \rho b_3 = \rho \frac{\partial^2 u_3}{\partial t^2}, \tag{2.12}$$

and

$$\frac{\partial \sigma_{11}}{\partial x_1} + \frac{\partial \sigma_{12}}{\partial x_2} + \rho b_1 = \rho \frac{\partial^2 u_1}{\partial t^2},$$

$$\frac{\partial \sigma_{21}}{\partial x_1} + \frac{\partial \sigma_{22}}{\partial x_2} + \rho b_2 = \rho \frac{\partial^2 u_2}{\partial t^2}.$$

(2.13)

Motion, corresponding to the displacement $u_3(x_1, x_2, t)$ is known as the antiplane or out of plane motion, while the displacements u_1 and u_2 are associated with plane strain deformation.

In what follows we study the antiplane motion, starting from the equation (2.12), where we can use u instead of u_3 without ambiguity. The stress components of interest are expressed through the Hooke's Law as

$$\sigma_{13} = \mu \frac{\partial u}{\partial x_1}, \qquad \sigma_{23} = \mu \frac{\partial u}{\partial x_2}.$$

(2.14)

Therefore, in absence of body forces, the scalar wave equation for $u(x_1, x_2, t)$ becomes

$$\frac{\partial^2 u}{\partial x_1^2} + \frac{\partial^2 u}{\partial x_2^2} = \frac{1}{c_2^2} \frac{\partial^2 u}{\partial t^2},$$

(2.15)

where $c_2 = \sqrt{\frac{\mu}{\rho}}$ is the shear wave speed; we also remark that compression wave speed is given by $c_1 = \sqrt{\frac{\lambda+2\mu}{\rho}}$.

For harmonic motions we have

$$u(x_1, x_2, t) = U(x_1, x_2)e^{i\omega t}, \tag{2.16}$$

where ω denotes the angular frequency. Then (2.15) can be re-written as

$$\frac{\partial^2 U}{\partial x_1^2} + \frac{\partial^2 U}{\partial x_2^2} + \frac{\omega^2}{c_2^2}U = 0, \tag{2.17}$$

where $U(x_1, x_2)$ is the magnitude of the out of plane displacement.

2.4 Concluding remarks

The presented fundamental relations including 2D equations for antiplane motion can be immediately adapted for the analysis of dynamic antiplane shear of layered laminates exposed in the subsequent chapters of the thesis. Extra basic formulae in linear elasticity, i.e. formulations of boundary-value problems as well as interfacial conditions for a perfect contact are introduced due to course below.

Chapter 3

Two-layered plate

Anti-plane dynamic shear of two-layered laminate is analysed for Neumann and Derichlet homogeneous boundary conditions along the upper and lower faces, respectively. The high contrast in stiffnesses and densities of the layers is considered; in doing so, the thicknesses of the layers are assumed to be of the same order. It is shown that for the studied contrast setup the value of the lowest cut-off frequency tends to zero. For this mode shortened dispersion relations and associated 1D equations of motion are derived. They appear to be valid over the whole low-frequency

range. Numerical data illustrating comparisons of exact and asymptotic results are

presented.

3.1   Statement of the problem
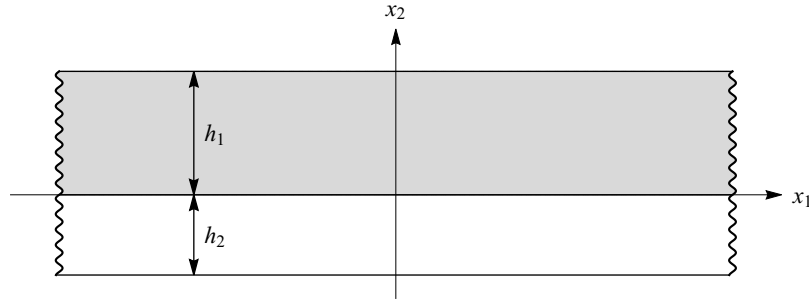
FIGURE 3.1:   Two-layered laminate

Consider dynamic anti-plane shear of a two-layered laminate with the thicknesses of

the upper and lower layers denoted by h_1 and h_2, respectively, see Figure 3.1. It is

assumed that the layers are linearly elastic and isotropic.

Then the equations of motion in Cartesian coordinates x_1, x_2 can be written as

$$\mu_q \Delta u_q = \rho_q u_{q,tt} \tag{3.1}$$

where u_q $(q = 1, 2)$ are out of plane displacements of q–th layer, t - time, $\Delta = \dfrac{\partial^2}{\partial x_1^2} + \dfrac{\partial^2}{\partial x_2^2}$ is 2D Laplacian, μ_q is Lame parameters and ρ_q is mass density.

The continuity conditions along the interface between the layers are

$$u_1 = u_2 \qquad \text{at} \qquad x_2 = 0, \tag{3.2}$$

$$\sigma_{32}^1 = \sigma_{32}^2 \qquad \text{at} \qquad x_2 = 0, \tag{3.3}$$

where σ_{32}^q are relevant shear stresses. Here and below

$$\sigma_{32}^q = \mu_q \frac{\partial u_q}{\partial x_2}. \tag{3.4}$$

We consider mixed fixed-free boundary conditions along the faces in the form

$$\sigma_{32}^1 = 0 \qquad \text{at} \qquad x_2 = h_1, \tag{3.5}$$

$$u_2 = 0 \qquad \text{at} \qquad x_2 = -h_2. \tag{3.6}$$

3.2   Dispersion relation

We seek solutions of the formulated above problem in the form of the travelling wave

$$u_q = f_q(x_2)e^{i(kx_1 - \omega t)}, \quad q = 1, 2, \tag{3.7}$$

where k is the wave number and ω is the frequency. Substituting the latter into equations of motion (3.1) we arrive at

$$\frac{\partial^2 f_q}{\partial x_2^2} + f_q \left(\frac{\omega^2}{c_{2q}^2} - k^2 \right) = 0, \tag{3.8}$$

where $c_{2q} = \sqrt{\mu_q / \rho_q}$. As a result, we obtain the functions f_q in the form

$$f_q(x_2) = A_q \cosh \left(\sqrt{k^2 - \frac{\omega^2}{c_{2q}^2}} x_2 \right) + B_q \sinh \left(\sqrt{k^2 - \frac{\omega^2}{c_{2q}^2}} x_2 \right). \tag{3.9}$$

Now applying boundary conditions and continuity relations stated in the previous section, we obtain a system of four equations in four unknowns A_1, A_2, B_1, B_2. This system has a non-trivial solution provided

$$\begin{vmatrix} 0 & \mu_1 \phi_1 & 0 & -\mu_2 \phi_2 \\ 1 & 0 & -1 & 0 \\ \mu_1 \phi_1 S_1 & \mu_1 \phi_1 C_1 & 0 & 0 \\ 0 & 0 & C_2 & -S_2 \end{vmatrix} = 0, \tag{3.10}$$

where

$$S_q = \sinh(\phi_q h_q), \quad C_q = \cosh(\phi_q h_q), \tag{3.11}$$

and

$$\phi_{\mathrm{q}} = \sqrt{\mathrm{k}^2 - \frac{\omega^2}{\mathrm{c}_{2\mathrm{q}}^2}}, \qquad \mathrm{q} = 1, 2. \tag{3.12}$$

Equation (3.10) yields a dispersion relation in the form

$$\mu_2\phi_1\left[\mu_2\phi_2\mathrm{C}_1\mathrm{C}_2 + \mu_1\phi_1\mathrm{S}_1\mathrm{S}_2\right] = 0. \tag{3.13}$$

The obtained dispersion relation can also be re-written in dimensionless form as

$$\mu\alpha_1\cosh(\alpha_1)\cosh(\alpha_2\mathrm{h}) + \alpha_2\sinh(\alpha_1)\sinh(\alpha_2\mathrm{h}) = 0, \tag{3.14}$$

where

$$\alpha_1 = \sqrt{\mathrm{K}^2 - \Omega^2}, \qquad\qquad \alpha_2 = \sqrt{\mathrm{K}^2 - \frac{\mu}{\rho}\Omega^2}. \tag{3.15}$$

Non-dimensional frequency Ω and wavenumber K are introduced as

$$\Omega = \frac{\omega\mathrm{h}_2}{\mathrm{c}_{22}}, \qquad\qquad \mathrm{K} = \mathrm{kh}_2, \tag{3.16}$$

with

$$h = \frac{h_1}{h_2}, \qquad \mu = \frac{\mu_2}{\mu_1}, \qquad \rho = \frac{\rho_2}{\rho_1}, \qquad c_{2q} = \sqrt{\frac{\mu_q}{\rho_q}}, \qquad q = 1, 2. \qquad (3.17)$$

Dispersion curves, computed from the dispersion relation above, are plotted in Figures 3.2 and 3.3 for non-contrast and contrast cases. Due to a contrast in density and stiffness of the layers, the first harmonic cut-off in Figure 3.3 is less than that in Figure 3.2.
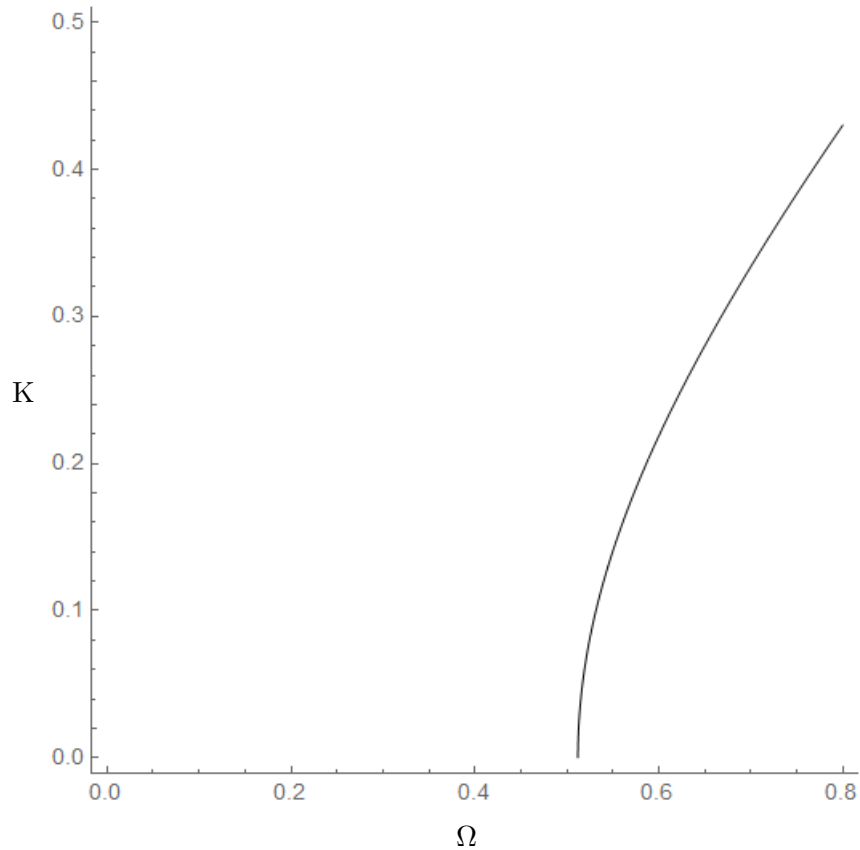
FIGURE 3.2: Dispersion curve for (3.14) for $h = 1.0$, $\mu = 0.6$ and $\rho = 3.0$.
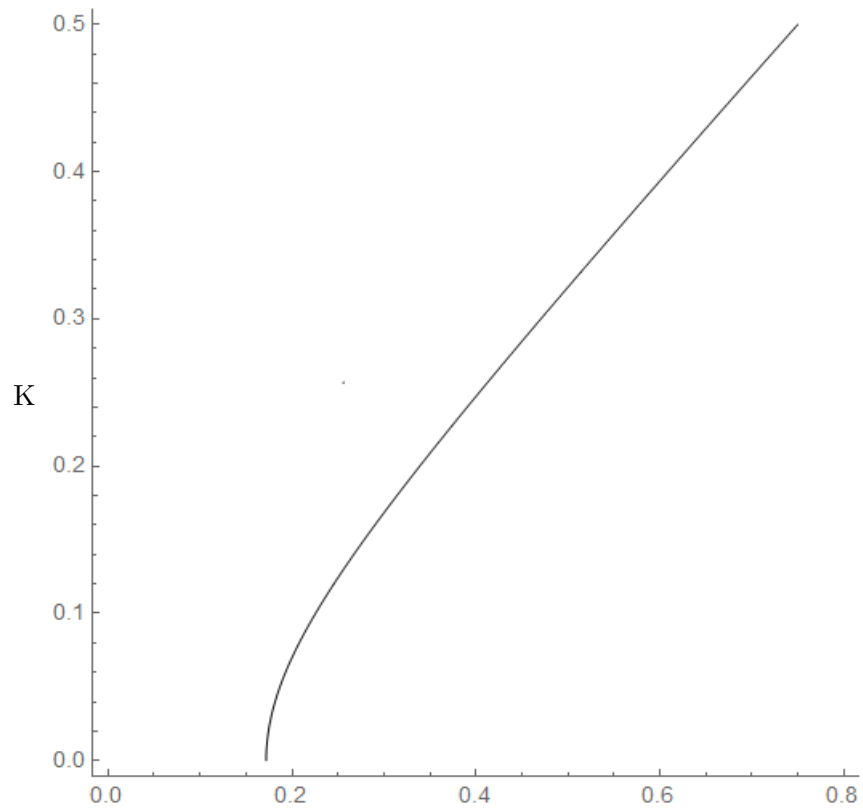
FIGURE 3.3: Dispersion curves (3.14) for h = 1.0, $\mu = 0.014$ and $\rho = 0.32$.

3.3   Asymptotic approximations

Here we study the parameter setup for which

$$\mu \ll 1, \qquad h \sim 1, \qquad \rho \sim \mu. \tag{3.18}$$

The equation for cut-off frequency follows from the dispersion relation (3.14) at K = 0.

It is given by

$$\tan\left(h\Omega\sqrt{\frac{\mu}{\rho}}\right)\tan\Omega = \sqrt{\mu\rho}. \tag{3.19}$$

The chosen set of parameters (3.18) corresponds to the so-called global low-frequency

regime, see for example Kaplunov et al. [2017a]

$$\rho \ll h \ll \mu^{-1}, \tag{3.20}$$

giving for leading order for a single low-frequency cut-off

$$\Omega \approx \sqrt{\frac{\rho}{h}} \ll 1. \tag{3.21}$$

Consider the long-wave low-frequency limit

$$\mathrm{K} \ll 1, \qquad\qquad\qquad \Omega \ll 1. \qquad\qquad (3.22)$$

Then, we expand trigonometric functions in (3.14) into asymptotic series, resulting

in the polynomial dispersion relation

$$\gamma_0 + \mathrm{K}^2\gamma_1 + \Omega^2\gamma_2 + \mathrm{K}^2\gamma_3 + \Omega^4\gamma_4 + \Omega^2\mathrm{K}^2\gamma_5 + ... = 0, \qquad (3.23)$$

where γ_i are coefficients depending on dimensionless problem parameters ρ, μ, h. In

the polynomial dispersion relation above

$$
\begin{aligned}
\gamma_1 &= \frac{\mathrm{h}^2\mu}{2} + \mathrm{h} + \frac{\mu}{2}, \\[6pt]
\gamma_2 &= \frac{\mathrm{h}^4\mu}{24} + \frac{\mathrm{h}^3}{6} + \frac{\mathrm{h}^2\mu}{4} + \frac{\mathrm{h}}{6} + \frac{\mu}{24}, \\[6pt]
\gamma_3 &= -\frac{\mathrm{h}^4\mu^2}{12\rho} - \frac{\mathrm{h}^3\mu}{3\rho} - \frac{\mathrm{h}^2\mu^2}{4\rho} - \frac{\mathrm{h}^2\mu}{4} - \frac{\mathrm{h}\mu}{6\rho} + \frac{\mathrm{h}}{6} - \frac{\mu}{12}, \\[6pt]
\gamma_4 &= -\frac{\mathrm{h}^2\mu^2}{2\rho} - \frac{\mathrm{h}\mu}{\rho} - \frac{\mu}{2}, \\[6pt]
\gamma_5 &= \frac{\mathrm{h}^4\mu^3}{24\rho^2} + \frac{\mathrm{h}^3\mu^2}{6\rho^2} + \frac{\mathrm{h}^2\mu^2}{4\rho} + \frac{\mathrm{h}\mu}{6\rho} + \frac{\mu}{24}.
\end{aligned}
\qquad (3.24)
$$

At leading order these coefficients are given below

$$\gamma_1^0 = \mathrm{h},$$

$$\gamma_2^0 = \frac{1}{6}\left(\mathrm{h}^3 + \mathrm{h}\right),$$

$$\gamma_3^0 = \frac{-2\mathrm{h}^3 - \mathrm{h}\rho_\mu - \mathrm{h}}{6\rho_\mu}, \qquad (3.25)$$

$$\gamma_4^0 = -\frac{\mathrm{h}}{\rho_\mu},$$

$$\gamma_5^0 = \frac{\mathrm{h}^3 + \mathrm{h}\rho_\mu}{6\rho_\mu^2},$$

where $\rho_\mu = \rho/\mu \sim 1$.

Thus, for the chosen contrast we have

$$\gamma_0 \sim \gamma_1 \sim \gamma_2 \sim \gamma_3 \sim \gamma_4 \sim \gamma_5 \sim 1,$$

leading to the shortened dispersion relation

$$\frac{\mu}{\mathrm{h}} + \mathrm{K}^2 - \frac{\mu}{\rho}\Omega = 0. \qquad (3.26)$$

The derived approximate dispersion relation for the long-wave low-frequency regime demonstrates good agreement with the numerical implementation of the exact solution, see Figure 3.4. In this figure solid line denotes exact solution, while dashed one
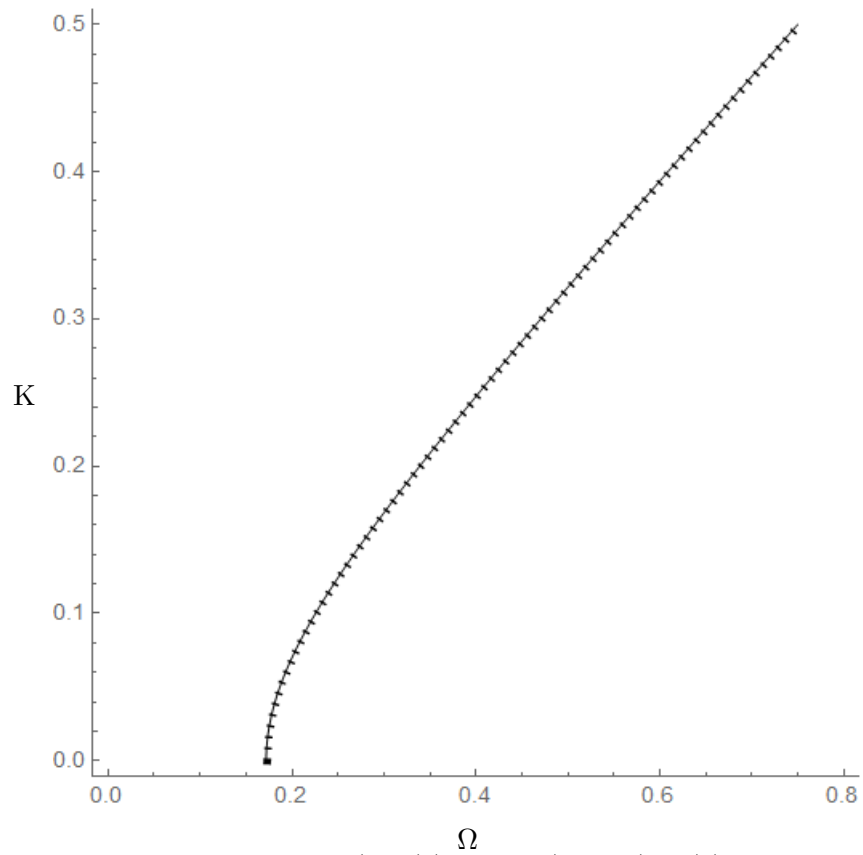
FIGURE 3.4: Dispersion curves (3.14)(solid line) and (3.26)(dotted lines) for h = 1.0, $\mu = 0.01$ and $\rho = 0.03$.

corresponds to the shortened dispersion relation.

3.4   Derivation of approximate equation of motion

First, scale longitudinal coordinate and time by

$$x_1 = \frac{h_1}{\sqrt{\mu}}\xi_1$$

and

$$t = \frac{h_1}{c_{21}\sqrt{\mu}}\tau,$$

motivated by the asymptotic analysis of the associated dispersion relation. Also,

introduce the dimensionless transverse coordinate as

$$x_2 = h_1\xi_{21}, \quad 0 < x_2 < h_1,$$

$$x_2 = h_2\xi_{22} + h_1, \quad h_1 < x_2 < h_1 + h_2.$$

Then, displacements and stresses are

$$u_q = h_1 v_q, \quad \sigma_{13}^q = \mu_q\sqrt{\mu}s_{13}^q, \quad \sigma_{23}^q = \mu_1 s_{23}^q, \quad q = 1, 2, \tag{3.27}$$

where v_q, s_{13}^q, s_{23}^q assumed of $O(1)$.

Prior proceeding with asymptotic analysis re-write the governing equations above in

the form

$$\frac{\partial \sigma_{13}^q}{\partial x_1} + \frac{\partial \sigma_{23}^q}{\partial x_2} - \rho_q \frac{\partial^2 u_q}{\partial t^2} = 0, \tag{3.28}$$

$$\sigma_{i3}^q = \mu_q \frac{\partial u_q}{\partial x_i}, \quad i, q = 1, 2.$$

In the dimensionless form the latter become

$$\mu \frac{\partial s_{13}^1}{\partial \xi_1} + \frac{\partial s_{23}^1}{\partial \xi_{21}} - \mu \frac{\partial^2 v_1}{\partial \tau^2} = 0, \tag{3.29}$$

and

$$\frac{\partial s_{13}^2}{\partial \xi_1} + \frac{1}{h} \frac{\partial s_{23}^2}{\partial \xi_{22}} - \frac{1}{\rho_\mu} \frac{\partial^2 v_2}{\partial \tau^2} = 0, \tag{3.30}$$

where $\rho_\mu = \rho/\mu$ and

$$s_{23}^2 = \frac{1}{\mu h} \frac{\partial v_2}{\partial \xi_{22}}, \qquad s_{13}^2 = \frac{\partial v_2}{\partial \xi_1}. \tag{3.31}$$

The related continuity conditions are

$$v_1|_{\xi_{21}=1} = v_2|_{\xi_{22}=0} \tag{3.32}$$

and

$$s^1_{23}\big|_{\xi_{21}=1} = \mu s^2_{23}\big|_{\xi_{22}=0}. \tag{3.33}$$

Finally, the imposed mixed face boundary conditions are written as

$$s^2_{23}\big|_{\xi_{22}=1} = 0, \qquad v_1\big|_{\xi_{12}=0} = 0. \tag{3.34}$$

Now, expand the dimensionless quantities v_q and s^q_{j2} in asymptotic series in small μ.

We get

$$v_q = v_{q,0} + \mu v_{q,1} + \cdots, \tag{3.35}$$

$$s^q_{j2} = s^q_{j2,0} + \mu s^q_{j2,1} + \cdots, \quad q = 1, 2, \qquad j = 1, 2.$$

At leading order we have

$$\frac{\partial s_{23,0}^1}{\partial \xi_{21}} = 0,$$

$$s_{13,0}^1 = \frac{\partial v_{1,0}}{\partial \xi_1}, \qquad s_{23,0}^1 = \frac{\partial v_{1,0}}{\partial \xi_{21}},$$

$$\frac{\partial s_{13,0}^2}{\partial \xi_1} + \frac{1}{h}\frac{\partial s_{23,0}^2}{\partial \xi_{22}} - \frac{1}{\rho_\mu}\frac{\partial^2 v_{2,0}}{\partial \tau^2} = 0,$$

$$s_{13,0}^2 = \frac{\partial v_{2,0}}{\partial \xi_1}, \qquad \frac{\partial v_{2,0}}{\partial \xi_{22}} = 0. \tag{3.36}$$

$$v_{1,0}|_{\xi_{21}=1} = v_{2,0}|_{\xi_{22}=0}$$

$$s_{23,0}^1|_{\xi_{21}=1} = s_{23,0}^2|_{\xi_{22}=0}$$

$$s_{23,0}^2|_{\xi_{21}=1} = 0.$$

Thus, we have from the (3.36) in the equations above

$$v_{2,0} = w(\xi_1, \tau). \tag{3.37}$$

Then, the rest of the quantities above is expressed in terms of $w(\xi_1, \tau)$ becoming

$$v_{1,0} = \xi_{21} w(\xi_1, \tau),$$

$$s_{13,0}^1 = \xi_{21}\frac{\partial w}{\partial \xi_1}, \qquad s_{13,0}^2 = \frac{\partial w}{\partial \xi_1}, \tag{3.38}$$

$$s_{23,0}^1 = w(\xi_1, \tau), \quad s_{23,0}^2 = (1 - \xi_{22})w,$$

with w satisfying the 1D equation

$$\frac{\partial^2 w}{\partial \xi_1^2} - \frac{1}{h} w - \frac{1}{\rho_\mu} \frac{\partial^2 w}{\partial \tau^2} = 0.$$ (3.39)

In terms of the original variables we have for $u_2(x_1, t) \approx w(x_1, t)$

$$\frac{\partial^2 u_2}{\partial x_1^2} - \frac{\rho_2}{\mu_2} \frac{\partial^2 u_2}{\partial t^2} - \frac{\mu_1 h_1}{\mu_2 h_1 h_2} u_2 = 0.$$ (3.40)

Now insert $u_2 = e^{i(kx_1 - \omega t)}$ into the last equation having

$$k^2 - \frac{\rho_2}{\mu_1} \omega^2 + \frac{\mu_1}{\mu_2 h_1 h_2} = 0.$$ (3.41)

This is the same as shortened dispersion equation (3.26), presented in dimensionless form.

3.5   Concluding remarks

In conclusion of this chapter we mention that all of the obtained results are in agreement with the consideration in Prikazchikova et al. [2020], dealing with antisymmetric antiplane shear of a three-layered laminate. In the latter case the even out of plane displacement takes a zero value along the middle line. As a result, the mixed boundary conditions (3.5) and (3.6), adapted in this chapter, are satisfied for a three-layered symmetric structure as well.

Thus, the problem considered in this chapter is in fact a toy one aiming at establishing the general methodology implemented in what follows for tackling a novel setup of an asymmetric three-layered laminate. In particular, first we study the long-wave low-frequency asymptotic limit of the full dispersion relation. Then, the scaling determined are applied for the derivation of the associated 1D shortened equations of motion. In this case, in contrast to one-mode asymptotic analysed in this chapter, the rest of the thesis is concerned with two-mode ones. The latter also involve the fundamental vibration mode in addition to the lowest shear harmonic considered above.

Chapter 4

Dispersion of antiplane shear

waves in a three-layered plate

The anti-plane shear of a three-layered laminate of an asymmetric structure is considered. The chosen geometry of the laminate assumes coupling its symmetric and anti-symmetric vibration modes, which is not a feature of a symmetric structure, see Prikazchikova et al. [2020]. As in the previous chapter, high contrast in mechanical properties of the inner and outer layers is assumed. A specific contrast setup supporting an asymptotically small lowest shear cut-off frequency is studied. Traction free boundary conditions are imposed on the faces. The conditions of the perfect

contact between layers are considered.

The exact dispersion relation of the problem is obtained. Two-mode long-wave low-frequency approximation of this dispersion relation incorporating both the fundamental mode and the first harmonic is derived. The accuracy of the derived approximations is tested by numerical comparison with the exact solution.

4.1   Statement of the problem

Consider a three-layered asymmetric laminate with isotropic layers of thickness h_1, h_2 and h_3, see Figure 4.1. The Cartesian coordinate system (x_1, x_2) is chosen in such a way that the axis x_1 goes through the mid-plane of the core layer. Two outer layers are assumed to have the same material parameters.

For the antiplane shear deformation the equations of motion for each layer can be written as

$$\frac{\partial \sigma_{13}^l}{\partial x_1} + \frac{\partial \sigma_{23}^l}{\partial x_2} - \rho_l \frac{\partial^2 u_l}{\partial t^2} = 0, \qquad l = 1, 2, 3, \tag{4.1}$$

with

$$\sigma_{i3}^l = \mu_l \frac{\partial u_l}{\partial x_i}, \quad i = 1, 2, \tag{4.2}$$
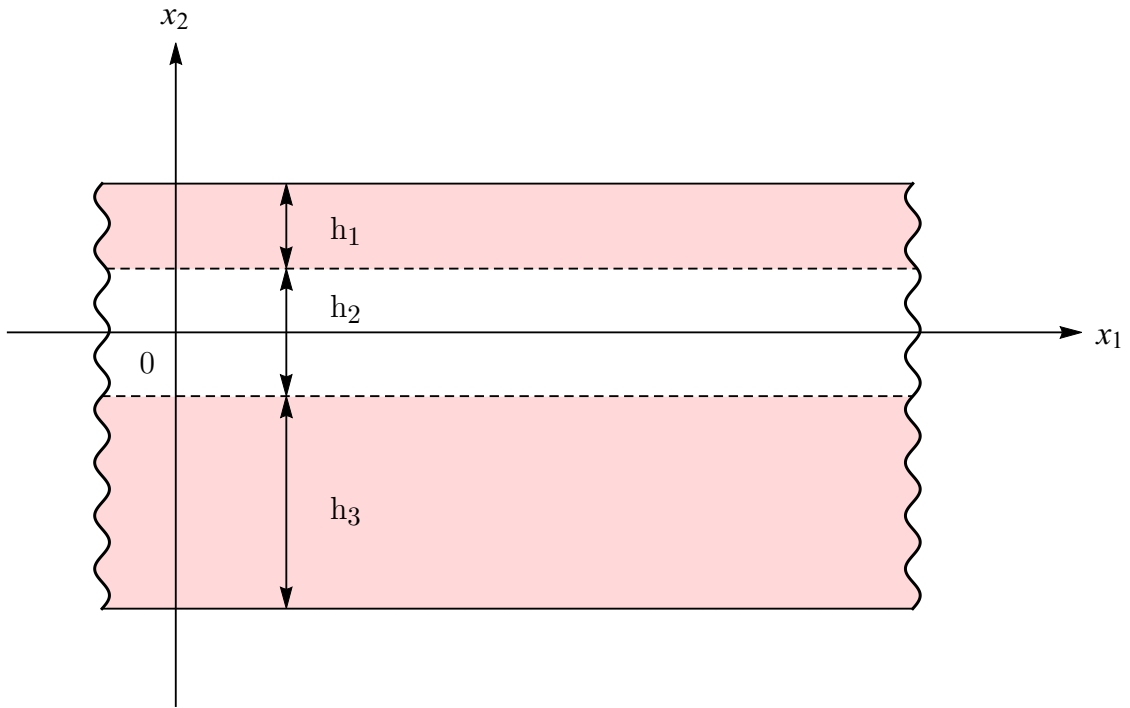
FIGURE 4.1: A three-layered asymmetric plate

where σ_{i3}^l are shear stresses, $u_l = u_l(x_1, x_2)$ are out of plane displacements, t is time,

μ_l are Lamé parameters, and ρ_l are mass densities. As we have already mentioned,

$\mu_1 = \mu_3$ and $\rho_1 = \rho_3$.

The continuity and traction-free boundary conditions are given by

$$u_1 = u_2, \quad \sigma_{23}^1 = \sigma_{23}^2 \quad \text{at} \quad x_2 = \frac{h_2}{2},$$

$$u_2 = u_3, \quad \sigma_{23}^2 = \sigma_{23}^3 \quad \text{at} \quad x_2 = -\frac{h_2}{2},$$

(4.3)

and

$$
\sigma_{23}^1 = 0 \quad \text{at} \quad x_2 = \frac{h_2}{2} + h_1,
$$

$$
\sigma_{23}^3 = 0 \quad \text{at} \quad x_2 = -\frac{h_2}{2} - h_3,
$$

(4.4)

respectively.

4.2 Dispersion relation

We proceed in a way, similar to two-layered plate, although in this case we need to take into account three layers. We seek solutions of the formulated above problem (4.1)-(4.4) in the form of the travelling wave

$$
u_q = f_q(x_2) e^{i(kx_1 - \omega t)}, \quad q = 1, 2,
$$

(4.5)

where k is the wave number and ω is the frequency. Substituting the latter into equations of motion (4.1) we arrive at

$$
\frac{\partial^2 f_q}{\partial x_2^2} + f_q \left(\frac{\omega^2}{c_{2q}^2} - k^2 \right) = 0,
$$

(4.6)

where $c_{2q} = \sqrt{\mu_q/\rho_q}$, $q = 1, 2, 3$. As a result, we obtain the functions f_q in the form

$$f_q(x_2) = A_q \cosh\left(\sqrt{k^2 - \frac{\omega^2}{c_{2q}^2}}x_2\right) + B_q \sinh\left(\sqrt{k^2 - \frac{\omega^2}{c_{2q}^2}}x_2\right), \qquad q = 1, 2, 3. \quad (4.7)$$

Using boundary conditions (4.4) and continuity relations (4.3) we obtain a system of six equations in six unknowns A_q, B_q, $q = 1, 2, 3$. This system has a non-trivial solution provided the following determinant is zero

$$\begin{vmatrix} \mu_1\phi_1 S_1 & \mu_1\phi_1 C_1 & -\mu_2\phi_2 S_2 & -\mu_2\phi_2 C_2 & 0 & 0 \\ 0 & 0 & -\mu_2\phi_2 S_2 & \mu_2\phi_2 C_2 & \mu_1\phi_1 S_1 & -\mu_1\phi_1 C_1 \\ C_1 & S_1 & -C_2 & -S_2 & 0 & 0 \\ 0 & 0 & C_2 & -S_2 & -C_2 & S_1 \\ \mu_1\phi_1 SS_1 & \mu_1\phi_1 CC_1 & 0 & 0 & 0 & 0 \\ 0 & 0 & 0 & 0 & \mu_1\phi_1 SSS_1 & \mu_1\phi_1 CCC_1 \end{vmatrix} = 0 \quad (4.8)$$

where

$$S_q = \sinh(\phi_q(\frac{h_2}{2})), \qquad C_q = \cosh(\phi_q(\frac{h_2}{2})),$$

$$SS_q = \sinh(\phi_q(\frac{h_2}{2} + h_1)), \qquad CC_q = \cosh(\phi_q(\frac{h_2}{2} + h_1)), \qquad (4.9)$$

$$SSS_q = \sinh(\phi_q(\frac{-h_2}{2} - h_3)), \qquad CCC_q = \cosh(\phi_q(\frac{-h_2}{2} - h_3)),$$

and

$$\phi_q = \sqrt{k^2 - \frac{\omega^2 \rho_q}{\mu_q}} \qquad q = 1, 2. \tag{4.10}$$

Equation (4.8) provides the dispersion relation which can be represented in the explicit form

$$\mu_2 \cosh(h_3\phi_1) \left[\mu_1 \phi_1 \phi_2 \cosh(h_2\phi_2) \sinh(h_1\phi_1) + \mu_2 \phi_2{}^2 \cosh(h_1\phi_1) \sinh(h_2\phi_2) \right] +$$

$$\mu_1 \sinh(h_3\phi_1) \left[\mu_2 \phi_1 \phi_2 \cosh(h_1\phi_1) \cosh(h_2\phi_2) + \mu_1 \phi_1{}^2 \sinh(h_1\phi_1) \sinh(h_2\phi_2) \right] = 0$$

$$\tag{4.11}$$

The obtained dispersion relation (4.11) can also be re-written in dimensionless form as

$$\mu \alpha_1 \alpha_2 \big(\tanh(h_{12}\alpha_1) + \tanh(h_{32}\alpha_1) \big) + \mu^2 \alpha_2{}^2 \tanh(\alpha_2) +$$

$$+ \alpha_1{}^2 \tanh(h_{12}\alpha_1) \tanh(h_{32}\alpha_1) \tanh(\alpha_2) = 0 \tag{4.12}$$

where

$$\alpha_1 = \sqrt{K^2 - \frac{\mu}{\rho}\Omega^2}, \qquad \alpha_2 = \sqrt{K^2 - \Omega^2}, \tag{4.13}$$

and

$$K = kh_2, \qquad \Omega = \frac{\omega h_2}{c_2}, \qquad \mu = \frac{\mu_2}{\mu_1}, \qquad \rho = \frac{\rho_2}{\rho_1},$$

$$h_{12} = \frac{h_1}{h_2}, \qquad h_{32} = \frac{h_3}{h_2}, \tag{4.14}$$

with $c_2 = \sqrt{\mu_2/\rho_2}$.

Dispersion relation (4.12) can be reduced to a simpler one for a symmetric sandwich plate setting $h_1 = h_3$ and $h_2 = 2\tilde{h}_2$, e.g. see Prikazchikova et al. [2020]. Substituting these into above and introducing new notation $h = h_1/\tilde{h}_2$ we obtain a dispersion relation which can be factorised as

$$\big(2\mu\alpha_2 + \alpha_1 \tanh(\alpha_1 h) \tanh(\alpha_2)\big)\big(2\mu\alpha_2 \tanh(\alpha_2) + \alpha_1 \tanh(\alpha_1 h)\big) = 0. \tag{4.15}$$

The first and second aggregates in the left-hand side of (4.15) correspond to the dispersion relations for symmetric and antisymmetric waves, respectively, i.e they are

$$\big(2\mu\alpha_2 + \alpha_1 \tanh(\alpha_1 h) \tanh(\alpha_2)\big) = 0, \tag{4.16}$$

and

$$\big(2\mu\alpha_2 \tanh(\alpha_2) + \alpha_1 \tanh(\alpha_1 h)\big) = 0. \tag{4.17}$$

We also present the formulae for displacements

$$u_1 = 2\beta\mu\alpha_2 \cosh\left(\alpha_1\left(h_{12} + \frac{1}{2} - \xi\right)\right),$$

$$u_2 = \beta\left((\mu\alpha_2 + \alpha_1)\cosh\left(\alpha_1 h_{12} - \alpha_2\xi + \frac{\alpha_2}{2}\right)\right.$$

$$\left. +(\mu\alpha_2 - \alpha_1)\cosh\left(\alpha_1 h_{12} + \alpha_2\xi - \frac{\alpha_2}{2}\right)\right),$$

$$u_3 = \frac{\beta}{2\alpha_1}\left(-(\mu\alpha_2 - \alpha_1)^2\cosh\left(\alpha_1\left(h_{12} - \frac{1}{2} - \xi\right) - \alpha_2\right)\right. \tag{4.18}$$

$$+(\mu\alpha_2 + \alpha_1)^2\cosh\left(\alpha_1\left(h_{12} - \frac{1}{2} - \xi\right) + \alpha_2\right)$$

$$+(\mu^2\alpha_2^2 - \alpha_1^2)\cosh\left(\alpha_1\left(h_{12} + \frac{1}{2} + \xi\right) - \alpha_2\right)$$

$$\left. -(\mu^2\alpha_2^2 - \alpha_1^2)\cosh\left(\alpha_1\left(h_{12} + \frac{1}{2} + \xi\right) + \alpha_2\right)\right),$$

where $\xi = x_2/h_2$ is dimensionless vertical coordinate and

$$\beta = A\left((\mu\alpha_2 - \alpha_1)\sinh\left(\alpha_1 h_{12} - \frac{\alpha_2}{2}\right) - (\mu\alpha_2 + \alpha_1)\sinh\left(\alpha_1 h_{12} + \frac{\alpha_2}{2}\right)\right)^{-1},$$

with A being an arbitrary constant.

As an example we also plot in Figure 4.2 and Figure 4.3 the variation of properly normalised plate displacements u_i/β (4.18) across the thickness calculated at cut-off frequency (4.23), which takes the value $\Omega \approx 0.18$ for the same problems parameters as in Figure 4.11. For the fundamental mode in Figure 4.2 we have from (4.12)

$K \approx 0.13$, whereas for the first harmonic in Figure 4.3 we get $K = 0$.
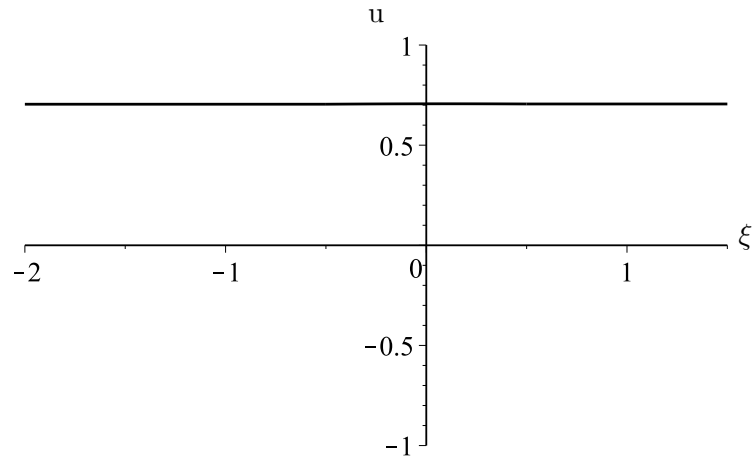
FIGURE 4.2: Displacement variations at the cut-off frequency $\Omega \approx 0.18$ for $h_{12} = 1.0$, $h_{32} = 1.5$, $\mu = 0.01$, and $\rho = 0.02$, fundamental mode
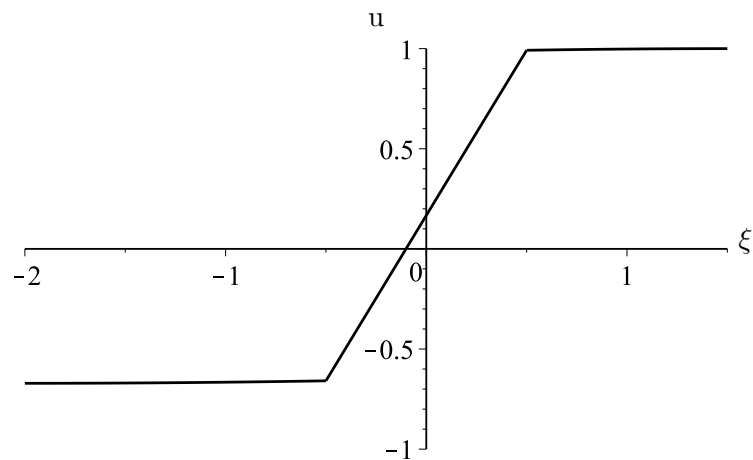
FIGURE 4.3: Displacement variations at the cut-off frequency $\Omega \approx 0.18$ for $h_{12} = 1.0$, $h_{32} = 1.5$, $\mu = 0.01$, and $\rho = 0.02$, first harmonic.

The next series of the graphs, see Figures 4.4-4.7, nicely illustrate a gradual transition from a high contrast setup to a more homogeneous one. At certain values of the problem parameters, see Figures 4.6-4.7, the analysed eigenform cannot be visually distinguished from a smooth one, characteristic of a single layer. We also note, that the cut-off frequency in all these graphs grows as the contrast diminishes according to the asymptotic considerations above. Similar illustrations could be also presented for the stresses.
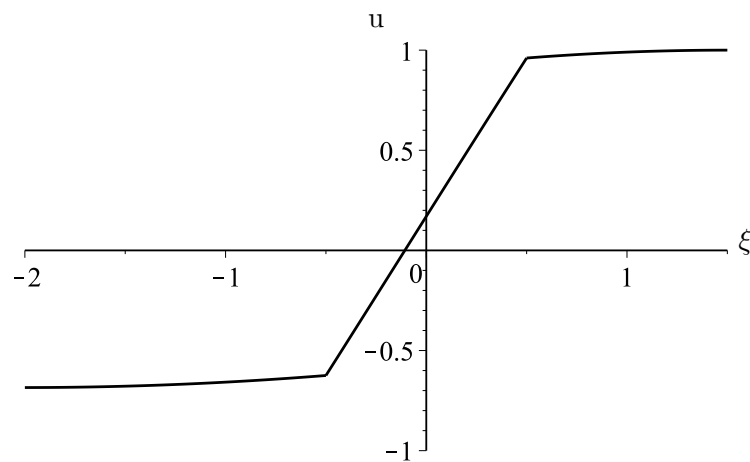
FIGURE 4.4: Displacement variations at the cut-off frequency $\Omega \approx 0.32$ for $h_{12} = 1.0$, $h_{32} = 1.5$, $\mu = 0.05$, and $\rho = 0.06$, first harmonic.
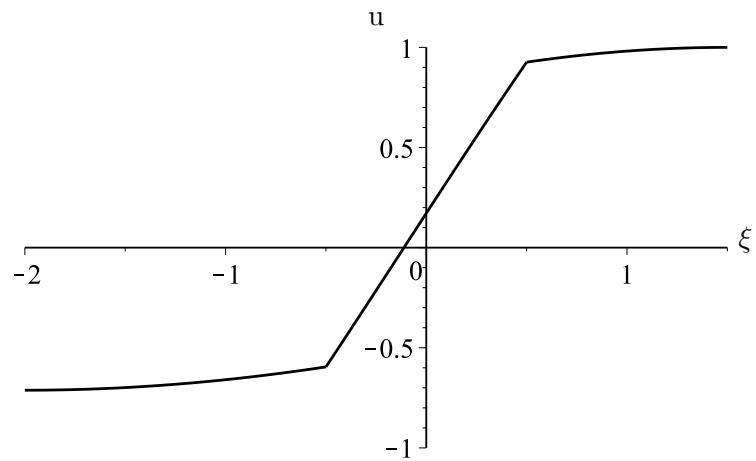
FIGURE 4.5: Displacement variations at the cut-off frequency $\Omega \approx 0.54$ for $h_{12} = 1.0$, $h_{32} = 1.5$, $\mu = 0.1$, and $\rho = 0.2$, first harmonic.
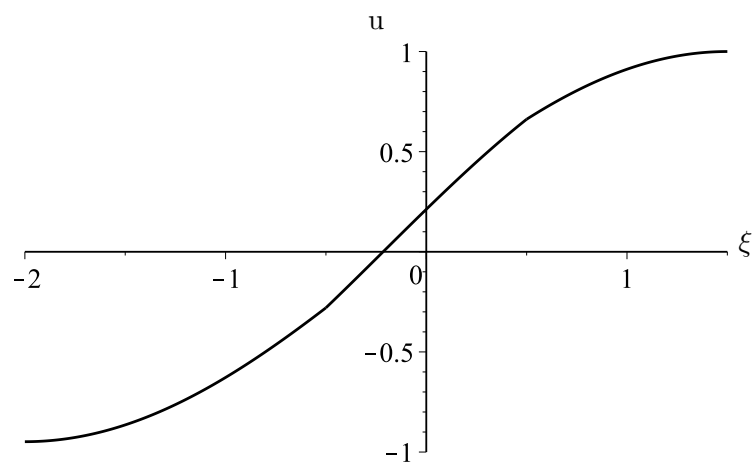
FIGURE 4.6: Displacement variations at the cut-off frequency $\Omega \approx 0.9$ for $h_{12} = 1.0$, $h_{32} = 1.5$, $\mu = 0.8$, and $\rho = 0.9$, first harmonic.
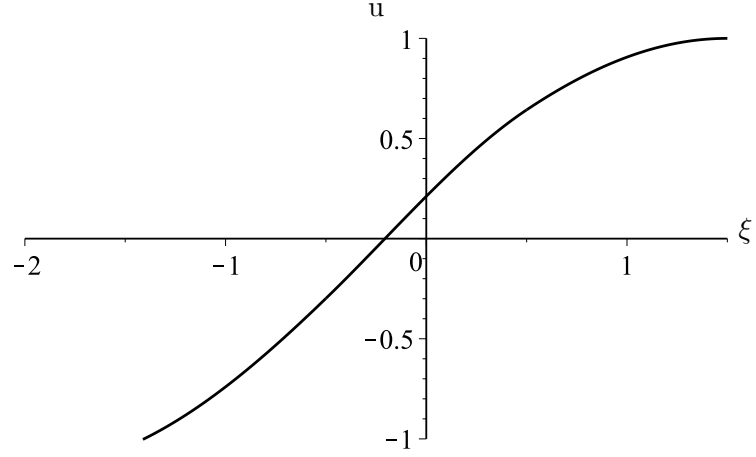
FIGURE 4.7: Displacement variations at the cut-off frequency $\Omega \approx 1.2$ for $h_{12} = 1.0$, $h_{32} = 1.5$, $\mu = 1.0$, and $\rho = 2.0$, first harmonic.

The related stresses are expressed as

$$\sigma_{23}^1 = \mu \alpha_1 \alpha_2 \beta_* \sinh\left(\alpha_1 \left(h_{12} - \xi + \frac{1}{2}\right)\right),$$

$$\sigma_{23}^2 = (\mu \alpha_2 \beta_*) \left(\mu^2 \cosh(h_{12}\alpha_1) \sinh\left(\alpha_2 \left(\frac{1}{2} - \xi\right)\right)\right.$$

$$\left. + \mu \alpha_1 \sinh(h_{12}\alpha_1) \cosh\left(\alpha_2 \left(\frac{1}{2} - \xi\right)\right)\right),$$

$$\sigma_{23}^3 = -\beta_* \left(\left(\mu \alpha_2 \cosh(\alpha_2) \cosh(h_{12}\alpha_1)\right.\right.$$

$$\left.\left. + \alpha_1 \sinh(\alpha_2) \sinh(h_{12}\alpha_1)\right)\left((\mu\alpha_1)\sinh\left(\alpha_1\left(h_{13} + \xi + \frac{1}{2}\right)\right)\right)\right),$$

$$(4.19)$$
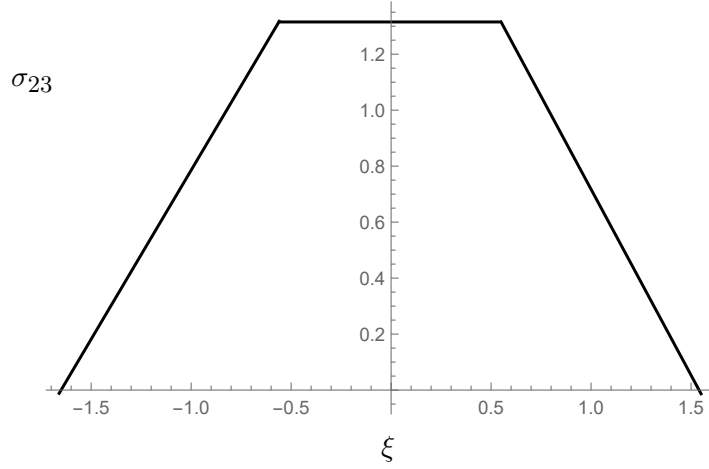
FIGURE 4.8: Normalized stresses σ_{23} computed from exact relations (4.19)

where $\xi = x_2/h_2$ and

$$\beta_* = \left(\mu \alpha_2 \cosh(h_{12}\alpha_1) \sinh\left(\frac{\alpha_2}{2}\right) + \alpha_1 \cosh\left(\frac{\alpha_2}{2}\right) \sinh(h_{12}\alpha_1) \right)^{-1} \qquad (4.20)$$

4.3   Shortened dispersion relation

First, setting $K = 0$ in dispersion relation (4.12), we have for the cut-off frequencies

$$\sqrt{\mu\rho} \left(\tan\left(h_{12}\sqrt{\frac{\mu}{\rho}}\Omega\right) + \tan\left(h_{32}\sqrt{\frac{\mu}{\rho}}\Omega\right) \right) + \mu\rho \tan\left(\Omega\right)$$

$$- \tan\left(h_{12}\sqrt{\frac{\mu}{\rho}}\Omega\right) \tan\left(h_{32}\sqrt{\frac{\mu}{\rho}}\Omega\right) \tan\left(\Omega\right) = 0. \qquad (4.21)$$

Consider the contrast in the material parameters of the outer and core layers given

by

$$\mu \ll 1, \quad \rho \sim \mu, \quad h_{12} \sim 1, \quad h_{32} \sim 1. \tag{4.22}$$

These formulae specify an asymmetric laminate with stiff outer layers and a soft

core. In this case, apart from usual zero cut-off ($\Omega = 0$) we have an extra small one

approximated by

$$\Omega \approx \sqrt{\frac{(h_{12} + h_{32})\rho}{h_{12}h_{32}}} \ll 1. \tag{4.23}$$

Hence, for the assumed contrast material properties we have two cut-offs over the

low frequency band. This is not the case for a non-contrast setup which allows only a

zero cut-off, corresponding to the fundamental symmetric mode. This observation is

illustrated numerically in Figure 4.9 and Figure 4.10 , where dispersion curves (4.12)

are plotted for both non-contrast and contrast setups.
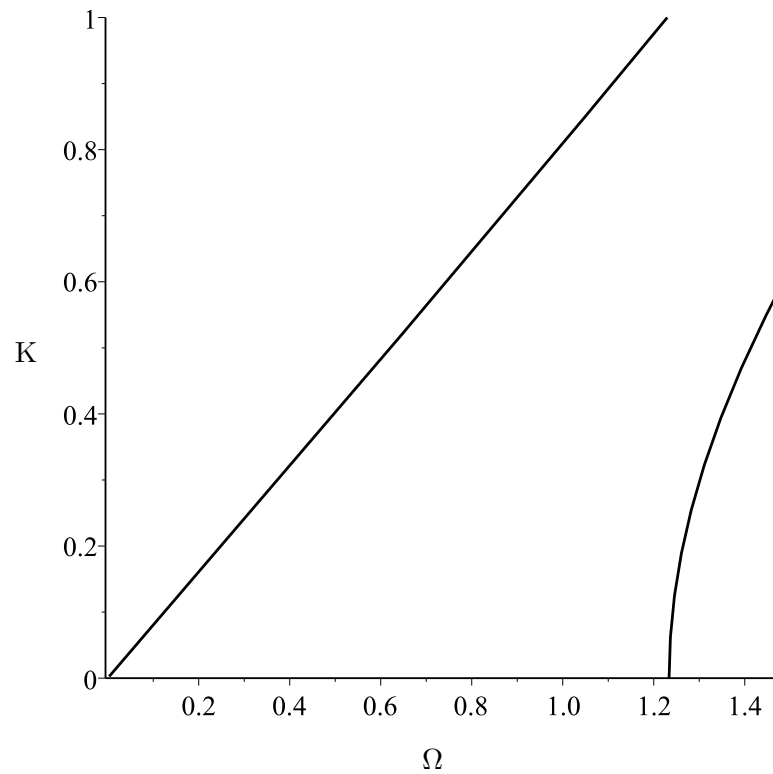
FIGURE 4.9: Dispersion curves (4.12) for $h_{12} = 1.0$, $h_{32} = 1.5$ and $\mu = 1.0$ and $\rho = 2.0$
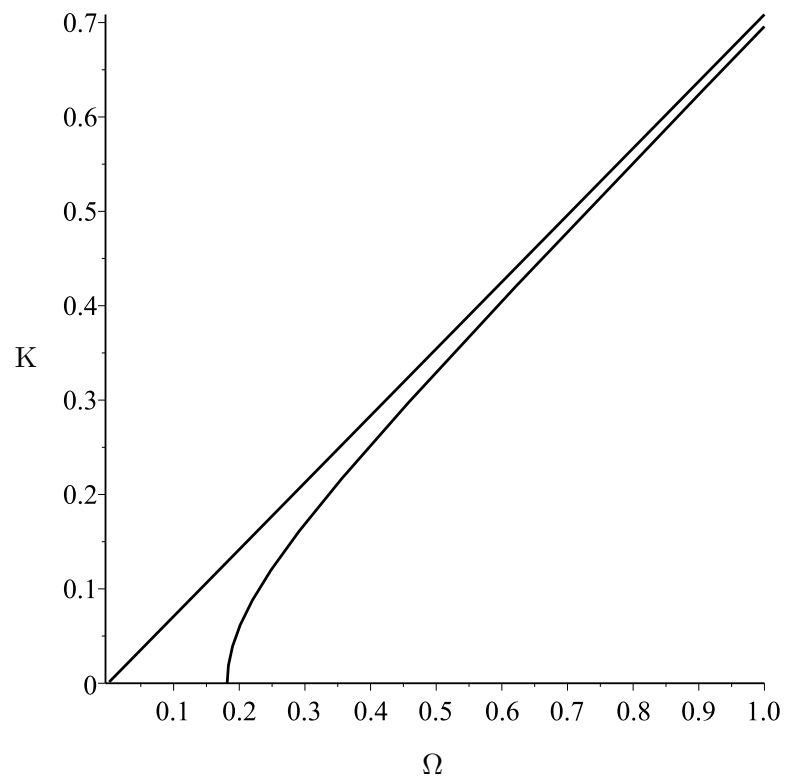
FIGURE 4.10: Dispersion curves (4.12) for $h_{12} = 1.0$, $h_{32} = 1.5$ and $\mu = 0.01$ and $\rho = 0.02$.

Next, expanding all trigonometric functions in (4.21) in asymptotic Taylor series at

$\Omega \ll 1$ and $K \ll 1$ and assuming relations (4.22) to be valid, we derive a polynomial

dispersion relation, which can be written as

$$\gamma_1 K^2 + \gamma_2 \Omega^2 + \gamma_3 K^4 + \gamma_4 K^2 \Omega^2 + \gamma_5 \Omega^4 + \gamma_6 K^6$$

$$+ \gamma_7 K^4 \Omega^2 + \gamma_8 K^2 \Omega^4 + \gamma_9 \Omega^6 + \cdots = 0, \quad (4.24)$$

where

$$\gamma_1 = \mu \left(h_{12} + h_{32} + \mu \right),$$

$$\gamma_2 = -\frac{\mu^2}{\rho} \left(h_{12} + h_{32} + \rho \right),$$

$$\gamma_3 = h_{12} h_{32} - \frac{\mu}{3} \left(h_{12}^3 + h_{32}^3 + \mu \right),$$

$$\gamma_4 = \frac{2\mu}{3\rho} \left(h_{12}^3 \mu + h_{32}^3 \mu - 3 h_{12} h_{32} + \mu \rho \right),$$

$$\gamma_5 = -\frac{\mu^2}{3\rho^2} \left(h_{12}^3 \mu + h_{32}^3 \mu - 3 h_{12} h_{32} + \rho^2 \right), \quad (4.25)$$

$$\gamma_6 = \frac{2\mu}{15} \left(h_{12}^5 + h_{32}^5 + \mu \right) - \frac{h_{12} h_{32}}{3} \left(h_{12}^2 + h_{32}^2 + 1 \right),$$

$$\gamma_7 = -\frac{1}{15\rho} \left(6\mu^2 \left(h_{12}^5 + h_{32}^5 + \rho \right) - 5 h_{12} h_{32} \left(3 h_{12}^2 \mu + 3 h_{32}^2 \mu + 2\mu + \rho \right) \right),$$

$$\gamma_8 = \frac{\mu}{15\rho^2} \left(6\mu \left(h_{12}^5 \mu + h_{32}^5 \mu + \rho^2 \right) - 5 h_{12} h_{32} \left(3 h_{12}^2 \mu + 3 h_{32}^2 \mu + \mu + 2\rho \right) \right),$$

$$\gamma_9 = -\frac{\mu^2}{15\rho^3} \left(2 \left(h_{12}^5 \mu^2 + h_{32}^5 \mu^2 + \rho^3 \right) - 5 h_{12} h_{32} \left(h_{12}^2 \mu + h_{32}^2 \mu + \rho \right) \right).$$

At leading order coefficients $\gamma_i \approx \gamma_i^0$ are given by

$$\gamma_1^0 = (h_{12} + h_{32})\,\mu,$$

$$\gamma_2^0 = -\frac{h_{12} + h_{32}}{\rho_\mu}\mu,$$

$$\gamma_3^0 = h_{12}h_{32},$$

$$\gamma_4^0 = -\frac{2h_{12}h_{32}}{\rho_\mu},$$

$$\gamma_5^0 = \frac{h_{12}h_{32}}{\rho_\mu^2}, \tag{4.26}$$

$$\gamma_6^0 = -\frac{h_{12}h_{32}}{3}\left(h_{12}^2 + h_{32}^2 + 1\right),$$

$$\gamma_7^0 = \frac{h_{12}h_{32}}{3\rho_\mu}\left(3h_{12}^2 + 3h_{32}^2 + \rho_\mu + 2\right),$$

$$\gamma_8^0 = -\frac{h_{12}h_{32}}{3\rho_\mu^2}\left(3h_{12}^2 + 3h_{32}^2 + 2\rho_\mu + 1\right),$$

$$\gamma_9^0 = \frac{h_{12}h_{32}}{3\rho_\mu^3}\left(h_{12}^2 + h_{32}^2 + \rho_\mu\right),$$

where $\rho_\mu = \rho/\mu$. From (4.26) we observe that $\gamma_1 \sim \gamma_2 \sim \mu$, and $\gamma_i \sim 1$, $i = 3,\ldots,9$. The leading order of each term in (4.24) can also be estimated for both the fundamental mode and the lowest harmonic. This data is presented in Table 4.1.

Order of γ_i	Terms	Fundamental mode $\Omega^2 \sim \mu K^2$	First harmonic $\Omega_{sh}^2 \sim \mu$
$\gamma_1 \sim \mu$	$\gamma_1 K^2$	μK^2	μK^2
$\gamma_2 \sim \mu$	$\gamma_2 \Omega^2$	μK^2	μ
$\gamma_3 \sim 1$	$\gamma_3 K^4$	μK^4	μK^4
$\gamma_4 \sim 1$	$\gamma_4 K^2 \Omega^2$	μK^4	μK^2
$\gamma_5 \sim 1$	$\gamma_5 \Omega^4$	μK^4	μ
$\gamma_6 \sim 1$	$\gamma_6 K^6$	μK^6	μK^6
$\gamma_7 \sim 1$	$\gamma_7 K^4 \Omega^2$	μK^6	μK^4
$\gamma_8 \sim 1$	$\gamma_8 K^2 \Omega^4$	μK^6	μK^2
$\gamma_9 \sim 1$	$\gamma_9 \Omega^6$	K^6	μK

TABLE 4.1: Asymptotic behaviour at $\mu \ll 1, \quad \rho \sim \mu, \quad h_{12} \sim h_{32} \sim 1$

As a result, the leading order shortened approximation, involving the fundamental mode with a zero cut-off along with the lowest harmonic with the cut-off of order $O(\sqrt{\mu})$ given by (4.23), takes the form

$$\gamma_1^0 K^2 + \gamma_2^0 \Omega^2 + \gamma_3^0 K^4 + \gamma_4^0 K^2 \Omega^2 + \gamma_5^0 \Omega^4 + \cdots = 0.$$

The above equation can be factorised as

$$\left(K^2\rho_\mu - \Omega^2\right)\left(h_{12}h_{32}\left(K^2\rho_\mu - \Omega^2\right) + \rho_\mu\mu(h_{12} + h_{32})\right) = 0. \qquad (4.27)$$

Therefore, for the fundamental mode and first harmonic we have

$$\Omega^2 = \rho_\mu K^2 \qquad (4.28)$$

and

$$\Omega^2 = \frac{\rho_\mu}{h_{12}h_{32}}\left(\mu(h_{12} + h_{32}) + h_{12}h_{32}K^2\right), \qquad (4.29)$$

respectively. It is worth mentioning that approximation (4.28) for the fundamental mode is valid over the whole low-frequency band $K \ll 1$, consequently, it does not fail at the vicinity of the cut-off (4.23), leading to a uniform approximation, see also Kaplunov et al. [2017a] concerned with a plane problem for three-layered symmetric laminate.

A numerical comparison is shown in Figure 4.11 for the exact dispersion curves (4.12) and approximations (4.28) and (4.29).
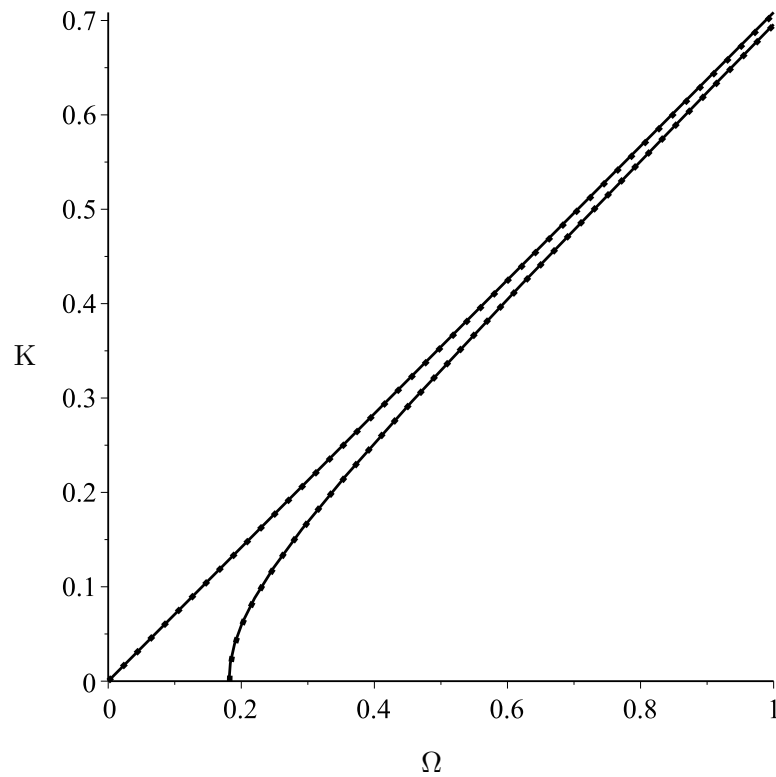
FIGURE 4.11: Dispersion curves (4.12) (solid line) together with approximations (4.28) and (4.29) (dotted lines) for $h_{12} = 1.0$, $h_{32} = 1.5$, $\mu = 0.01$, and $\rho = 0.02$.

4.4 Asymptotic formulae for displacements and stresses

Lets introduce variables ξ_{2i} (i $= 1, 2, 3$)

$$\xi_{21} = \frac{x_2}{h_1} - \frac{h_2}{2h_1},$$

$$\xi_{22} = \frac{x_2}{h_2} + \frac{1}{2}, \qquad (4.30)$$

$$\xi_{23} = \frac{x_2}{h_3} + \frac{h_2}{2h_3} + 1,$$

where $0 < \xi_{2i} < 1$. On inserting

$$K = K^*\sqrt{\mu}, \qquad \Omega = \Omega^*\sqrt{\mu}, \qquad K^* \sim \Omega^* \sim 1,$$

we get at leading order,

$$u_1 = \frac{\sqrt{\mu}\sqrt{K^{*2} - \Omega^{*2}\rho_\mu{}^{-1}}}{h_{12}\left(K^{*2} - \Omega^{*2}\right)}, \tag{4.31}$$

$$u_2 = \frac{\sqrt{\mu}\sqrt{K^{*2}\rho_\mu - \Omega^{*2}\rho_\mu{}^{-1}}\left(h_{12}K^{*2} - h_{12}\Omega^{*2} - 2h_{12}K^{*2} + 2h_{12}\xi_{22}\Omega^{*2} + 2h_{12}\right)}{2h_{12}\left(K^{*2} - \Omega^{*2}\right)}, \tag{4.32}$$

$$u_3 = \frac{\sqrt{\mu}\left(-h_{12}K^{*2} + h_{12}\Omega^{*2} - 1\right)\sqrt{K^{*2}\rho_\mu - \Omega^{*2}\rho_\mu{}^{-1}}}{h_{32}\left(K^{*2} - \Omega^{*2}\right)}, \tag{4.33}$$

$$\sigma_{23}^1 = \frac{\sqrt{\mu}\mu_2\left(h_{12} - \xi_{21} + \frac{1}{2}\right)\sqrt{K^{*2} - \Omega^{*2}\rho_\mu{}^{-1}}}{h_{12}}, \tag{4.34}$$

$$\sigma_{23}^2 = \frac{\mu^{3/2}\mu_1\sqrt{K^{*2}\rho_\mu - \Omega^{*2}\rho_\mu{}^{-1}}}{h_{12}}, \tag{4.35}$$

$$\sigma_{23}^3 = -\frac{\mu^{3/2}\mu_1\left(h_{12}K^{*2} - h_{12}\Omega^{*2} + 1\right)\left(h_{32} + \xi_{23} + \frac{1}{2}\right)\sqrt{K^{*2}\rho_\mu - \Omega^{*2}\rho_\mu{}^{-1}}}{h_{12}}. \tag{4.36}$$

4.5 Evanescent waves

Now, setting $\Omega = 0$, we deduce from (4.12) the static equation for K

$$
\begin{aligned}
\mathrm{K}^2 \Big(\mu \big(\tanh(\mathrm{h}_{12}\mathrm{K}) + \tanh(\mathrm{h}_{32}\mathrm{K}) \big) + \mu^2 \tanh(\mathrm{K}) + \\
+ \tanh(\mathrm{h}_{12}\mathrm{K}) \tanh(\mathrm{h}_{32}\mathrm{K}) \tanh(\mathrm{K}) \Big) = 0.
\end{aligned}
\tag{4.37}
$$

We have an obvious root $\mathrm{K} = 0$, associated with rigid body motion and another small one, given by

$$
\mathrm{K}^2 = \mathrm{K}_{\mathrm{bl}}^2 \approx -\frac{\mathrm{h}_{12} + \mathrm{h}_{32}}{\mathrm{h}_{12}\mathrm{h}_{32}} \mu \ll 1.
\tag{4.38}
$$

The latter is associated with slowly decaying boundary layers specific of high contrast laminates only, e.g. see Horgan [1998].

Figure 4.13 demonstrates dispersion curves including that corresponding to an evanescent wave for two sets of material parameters. In particular, Figure 4.12 is plotted for a laminate without contrast, while Figure 4.13 corresponds to a laminate with high contrast in material properties of the layers. The values of Ω_{sh} and K_{bl} are calculated using (4.23) and (4.38), respectively, for each set of parameters; here and below the lowest shear cut-off frequency Ω_{sh} is given by

$$
\Omega_{\mathrm{sh}} = \sqrt{\frac{(\mathrm{h}_{12} + \mathrm{h}_{32})\rho}{\mathrm{h}_{12}\mathrm{h}_{32}}}.
\tag{4.39}
$$

It can easily be observed that for the laminate with no contrast these values are of order 1, while for a high-contrast laminate they become small. In the case of Figure 4.12 the approximate values K_{bl} and Ω_{sh} do not provide even a rough estimation of the original values of these quantities, determined numerically.
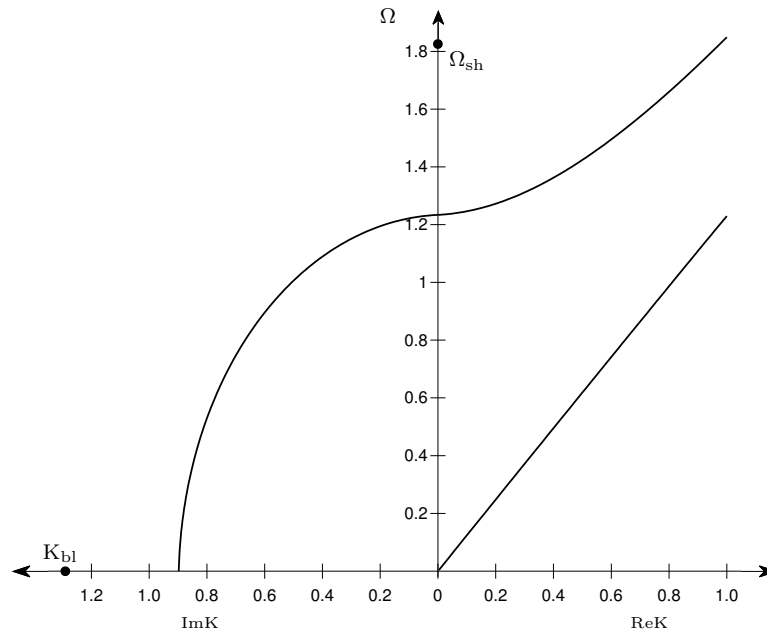
FIGURE 4.12: Numerical solution of dispersion relation (4.12) for $h_{12} = 1.0$, $h_{32} = 1.5$ and $\mu = 1.0$ and $\rho = 2.0$
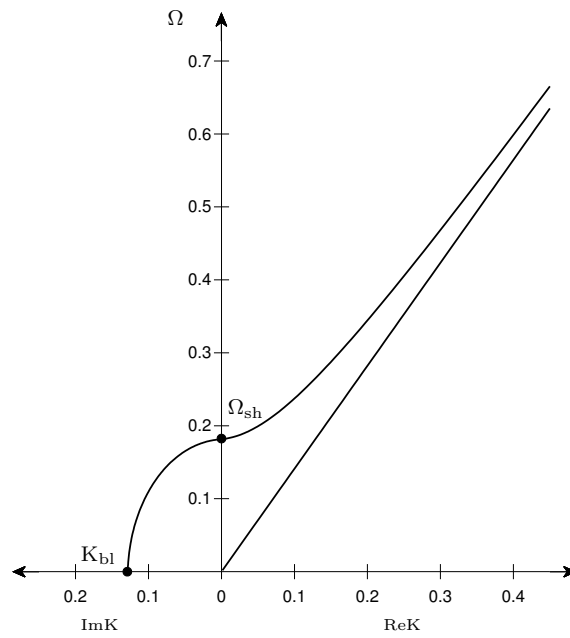
FIGURE 4.13: Numerical solution of dispersion relation (4.12) for $h_{12} = 1.0$, $h_{32} = 1.5$ and $\mu = 0.01$ and $\rho = 0.02$.

We also note that if $K = 0$ in (4.29) than we arrive at the expression for the cut-off frequency (4.39), which is of order $\sqrt{\mu}$. Alternatively, setting $\Omega = 0$ in this equation, we get (4.38) for K. Hence, asymptotic formula (4.29) is valid for both quasi-static $(\Omega \ll \sqrt{\mu})$ and near cut-off $(\Omega \sim K \sim \sqrt{\mu})$ behaviour. Moreover, at $\sqrt{\mu} \ll K \ll 1$ it coincides at leading order with (4.28).
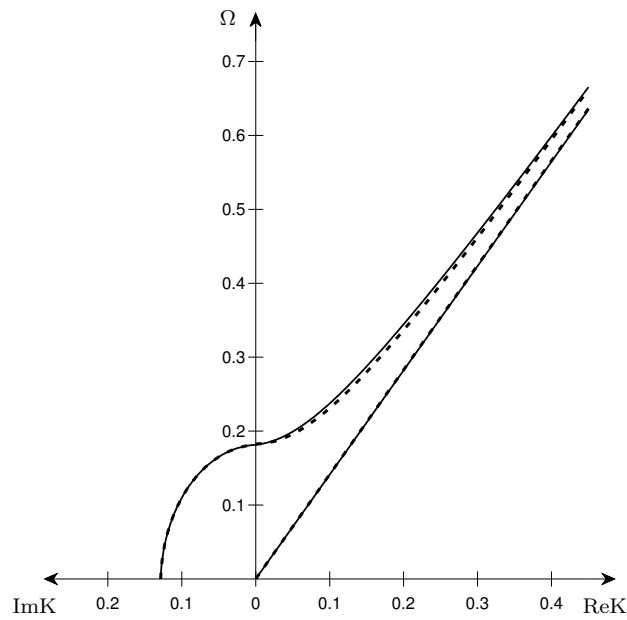
FIGURE 4.14: Numerical solution of dispersion relation (4.12)(solid line) together with asymptotic expansions (4.27) (dashed line) for $h_{12} = 1.0$, $h_{32} = 1.5$, $\mu = 0.01$ and $\rho = 0.02$.

Figure 4.14 demonstrates a good agreement between two exact dispersion curves

calculated from transcendental relation (4.12) and polynomial approximation (4.27)

for the chosen set of parameters

4.6 Concluding remarks

For the chosen high contrast scenario, in which the smallest shear cut-off frequency for a three-layered asymmetric laminate tends to zero, two low-frequency vibration modes, including the fundamental one and the first harmonic, are observed. These modes are evaluated from a shortened polynomial dispersion equation established in this chapter. This dispersion equation appears to be uniformly valid over the low-frequency range containing the first cut-off frequency.

Leading order asymptotic formulae for leading order displacements and stresses are also presented. In addition, the lowest evanescent mode having a long-wave static limit has been investigated in detail, including comparison of asymptotic and exact results.

Numerical comparison with the solutions of the full dispersion relation demonstrates a high accuracy of the derived two-mode asymptotic formula. The obtained explicit results have a clear potential to be extended to other types of contrast, as well as to plane vector problems. They also make an important preliminary insight to the essence of dynamic behaviour of high-contrast layered structures prior deriving long-wave partial differential models justifying which will be derived in the next chapter.

Chapter 5

Approximate equations of motion

and boundary conditions for a

three-layered plate

An asymmetric three-layered laminate with prescribed stresses along the faces is considered. The outer layers are assumed to be much stiffer than the inner one. The same type of contrast as in the previous chapter is assumed. The focus is on longwave low-frequency anti-plane shear.

The 1D equations of motion associated with the shortened dispersion relations derived in the previous chapter are split into two second-order operators in line with the factorisation of the mentioned dispersion relation. Asymptotically justified boundary conditions are established using the Saint-Venant's principle modified by taking into account the high-contrast properties of the laminate.

5.1   Statement of the problem

Consider a three-layered asymmetric plate defined in the previous section, see Figure 4.1. Hence, the equations of motion can be written as (4.1) and (4.2). All the notations and assumptions are the same as above. In particular, as we have already mentioned, $\mu_3 = \mu_1$ and $\rho_3 = \rho_1$.

The continuity and boundary conditions at the upper and lower faces are given by

([4.3](#)) and

$$
\begin{aligned}
\sigma_{23}^1 &= F_1 \quad \text{at} \quad x_2 = \frac{h_2}{2} + h_1, \\[2ex]
\sigma_{23}^3 &= F_3 \quad \text{at} \quad x_2 = -\frac{h_2}{2} - h_3,
\end{aligned}
\tag{5.1}
$$

respectively. Here F_1 and F_3 are prescribed forces.

5.2   Asymptotic derivation of 1D equations of mo-

tion

Introduce local dimensionless thickness variables ξ_{2i}, $i = 1, 2, 3$ in such a way that

they vary from 0 to 1 across each layer, i.e.

$$
\begin{aligned}
\xi_{21} &= \frac{1}{h_1}\left(x_2 - \frac{h_2}{2}\right), \\[2mm]
\xi_{22} &= \frac{1}{h_2}\left(x_2 + \frac{h_2}{2}\right), \\[2mm]
\xi_{23} &= \frac{1}{h_3}\left(x_2 + \frac{h_2}{2} + h_3\right).
\end{aligned}
\tag{5.2}
$$

From (4.28) it follows that $\Omega \sim K$. At the same time, (4.29) implies that $\Omega \sim K \sim$

$\sqrt{\mu}$. In the latter case both (4.28) and (4.29) are valid. Motivated by this observation,

we introduce the scaling

$$
x_1 = \frac{h_2}{\sqrt{\mu}}\xi_1, \qquad t = \frac{h_2}{c_{22}\sqrt{\mu}}\tau.
\tag{5.3}
$$

Then, the displacements and stresses can be normalised as

$$
u_q = h_2 v^q, \qquad \sigma_{13}^q = \mu_q\sqrt{\mu}S_{13}^q, \qquad \sigma_{23}^q = \mu_2 S_{23}^q, \quad q = 1, 2, 3.
\tag{5.4}
$$

The dimensionless form of the equations in the previous section for layers 1 and 3

$(q = 1, 3)$ can be written as

$$h_{q2}\frac{\partial S_{13}^q}{\partial \xi_1} + \frac{\partial S_{23}^q}{\partial \xi_{2q}} - \frac{h_{q2}}{\rho\mu}\frac{\partial^2 v^q}{\partial \tau^2} = 0, \tag{5.5}$$

$$S_{13}^q = \frac{\partial v^q}{\partial \xi_1}, \tag{5.6}$$

$$\mu h_{q2} S_{23}^q = \frac{\partial v^q}{\partial \xi_{2q}}, \tag{5.7}$$

while for layer 2 we get

$$\mu\frac{\partial S_{13}^2}{\partial \xi_1} + \frac{\partial S_{23}^2}{\partial \xi_{22}} - \mu\frac{\partial^2 v^2}{\partial \tau^2} = 0, \tag{5.8}$$

$$S_{13}^2 = \frac{\partial v^2}{\partial \xi_1}, \tag{5.9}$$

$$S_{23}^2 = \frac{\partial v^2}{\partial \xi_{22}}. \tag{5.10}$$

The continuity and boundary conditions become, respectively

$$v^1\big|_{\xi_{21}=0} = v^2\big|_{\xi_{22}=1}, \qquad v^2\big|_{\xi_{22}=0} = v^3\big|_{\xi_{23}=1},$$

$$S_{23}^1\big|_{\xi_{21}=0} = S_{23}^2\big|_{\xi_{22}=1}, \qquad S_{23}^2\big|_{\xi_{22}=0} = S_{23}^3\big|_{\xi_{23}=1}, \tag{5.11}$$

and

$$S_{23}^1\big|_{\xi_{21}=1} = \frac{F_1}{\mu_2} = f_1(\xi_1, \tau), \qquad S_{23}^3\big|_{\xi_{23}=0} = \frac{F_3}{\mu_2} = f_3(\xi_1, \tau). \tag{5.12}$$

Now expand displacements and stresses into asymptotic series in small parameter μ

$$v^q = v^q_0 + \mu v^q_1 + \dots,$$

$$S^q_{j3} = S^q_{j3,0} + \mu S^q_{j3,1} + \dots, \quad q = 1, 2, 3; \quad j = 1, 2. \tag{5.13}$$

At leading order we have for $q = 1, 3$

$$h_{q2} \frac{\partial S^q_{13,0}}{\partial \xi_1} + \frac{\partial S^q_{23,0}}{\partial \xi_{2q}} - \frac{h_{q2}}{\rho_\mu} \frac{\partial^2 v^q_0}{\partial \tau^2} = 0, \tag{5.14}$$

$$S^q_{13,0} = \frac{\partial v^q_0}{\partial \xi_1}, \tag{5.15}$$

$$\frac{\partial v^q_0}{\partial \xi_{2q}} = 0, \tag{5.16}$$

and for $q = 2$

$$\frac{\partial S^2_{23,0}}{\partial \xi_{22}} = 0, \quad S^2_{13,0} = \frac{\partial v^2_0}{\partial \xi_1}, \quad S^2_{23,0} = \frac{\partial v^2_0}{\partial \xi_{22}}. \tag{5.17}$$

Continuity relations (5.11) together with boundary conditions (5.12) become

$$v^1_0\big|_{\xi_{21}=0} = v^2_0\big|_{\xi_{22}=1}, \qquad v^2_0\big|_{\xi_{22}=0} = v^3_0\big|_{\xi_{23}=1}, \tag{5.18}$$

$$S^1_{23,0}\big|_{\xi_{21}=0} = S^2_{23,0}\big|_{\xi_{22}=1}, \qquad S^2_{23,0}\big|_{\xi_{22}=0} = S^3_{23,0}\big|_{\xi_{23}=1}, \tag{5.19}$$

$$S^1_{23,0}\big|_{\xi_{21}=1} = f_1, \qquad S^3_{23,0}\big|_{\xi_{23}=0} = f_3. \tag{5.20}$$

Next, we derive

$$v_0^1 = w_1(\xi_1, \tau), \quad v_0^3 = w_3(\xi_1, \tau), \quad v_0^2 = w_2\xi_{22} + w_3,$$

where

$$w_2 = w_1 - w_3.$$

Integrating equation (5.14) for q = 1 and q = 3, we obtain

$$S_{23,0}^1\big|_{\xi_{21}=0} = f_1 + h_{12}\left(\frac{\partial^2 w_1}{\partial \xi_1^2} - \frac{1}{\rho\mu}\frac{\partial^2 w_1}{\partial \tau^2}\right), \tag{5.21}$$

and

$$S_{23,0}^3\big|_{\xi_{23}=1} = f_3 - h_{32}\left(\frac{\partial^2 w_3}{\partial \xi_1^2} - \frac{1}{\rho\mu}\frac{\partial^2 w_3}{\partial \tau^2}\right). \tag{5.22}$$

Since

$$S_{23,0}^2 = \frac{\partial v_0^2}{\partial \xi_{22}} = w_2 = w_1 - w_3, \tag{5.23}$$

we can conclude that

$$S_{23,0}^1\big|_{\xi_{21}=0} = S_{23,0}^3\big|_{\xi_{23}=1} = w_1 - w_3 \tag{5.24}$$

resulting in the equations

$$w_1 - w_3 = f_1 + h_{12} \left(\frac{\partial^2 w_1}{\partial \xi_1^2} - \frac{1}{\rho_\mu} \frac{\partial^2 w_1}{\partial \tau^2} \right),$$

$$w_1 - w_3 = f_3 - h_{32} \left(\frac{\partial^2 w_3}{\partial \xi_1^2} - \frac{1}{\rho_\mu} \frac{\partial^2 w_3}{\partial \tau^2} \right).$$

(5.25)

Using the formulae above, we derive an equation for w_q, $q = 1, 3$. It is given by

$$\left(\rho_\mu \frac{\partial^2 w_q}{\partial \xi_1^2} - \frac{\partial^2 w_q}{\partial \tau^2} \right) \left(\rho_\mu (h_{12} + h_{32}) w_q - \right.$$

$$\left. h_{12} h_{32} \left(\rho_\mu \frac{\partial^2 w_q}{\partial \xi_1^2} - \frac{\partial^2 w_q}{\partial \tau^2} \right) \right) = 0,$$

(5.26)

and supports the same dispersion relation as (4.27) as might be expected.

In terms of stresses we have the equations

$$S_{23,0}^2 = f_1 + h_{12} \left(\frac{\partial S_{13,0}^1}{\partial \xi_1} - \frac{1}{\rho_\mu} \frac{\partial^2 w_1}{\partial \tau^2} \right),$$

$$S_{23,0}^2 = f_3 - h_{32} \left(\frac{\partial S_{13,0}^3}{\partial \xi_1} - \frac{1}{\rho_\mu} \frac{\partial^2 w_3}{\partial \tau^2} \right),$$

(5.27)

where

$$S_{13,0}^q = \frac{\partial w_q}{\partial \xi_1}, \quad q = 1, 3,$$

(5.28)

$$S_{23,0}^2 = w_2.$$

(5.29)

Thus,

$$\frac{\partial S_{13,0}^2}{\partial \xi_{22}} = S_{13,0}^1 - S_{13,0}^3. \tag{5.30}$$

In what follows, we also need the equations

$$\frac{\partial}{\partial \xi_1} \left(h_{12} S_{13,0}^1 + h_{32} S_{13,0}^3 \right) - \frac{1}{\rho \mu} \frac{\partial^2}{\partial \tau^2} \left(h_{12} w_1 + h_{32} w_3 \right) = f_3 - f_1,$$

$$\frac{\partial^2 S_{13,0}^2}{\partial \xi_1 \partial \xi_{22}} - \left(\frac{1}{h_{12}} + \frac{1}{h_{32}} \right) S_{23,0}^2 - \frac{1}{\rho \mu} \frac{\partial^2 w_2}{\partial \tau^2} = -\frac{f_3}{h_{32}} - \frac{f_1}{h_{12}}, \tag{5.31}$$

obtained as a linear combination of the equations in (5.27). Here, the first equation

corresponds to the outer stiff layers, while the second one governs the motion of the

soft middle layer.

5.3   Equations of motion in stress resultants and stress couples

As usual for thin plates and shells Kaplunov et al. [1998], Goldenveizer [2014], we define, starting from (5.4) and (5.13)

$$
N = \int_{h_2/2}^{h_2/2+h_1} \sigma_{13}^1 dx_2 + \int_{-h_2/2-h_3}^{-h_2/2} \sigma_{13}^3 dx_2
$$

$$
\approx \mu_1 \sqrt{\mu} \left(h_1 S_{13,0}^1 + h_3 S_{13,0}^3 \right),
$$

$$
T = \int_{-h_2/2}^{h_2/2} \sigma_{23}^2 dx_2 \approx h_2 \mu_2 S_{23,0}^2, \tag{5.32}
$$

$$
G = \int_{-h_2/2}^{h_2/2} \sigma_{13}^2 x_2 dx_2 \approx \mu_2 \sqrt{\mu} h_2^2 \int_0^1 S_{13,0}^2 \left(\xi_{22} - \frac{1}{2} \right) d\xi_{22}
$$

$$
= \frac{\mu_2 \sqrt{\mu} h_2^2}{12} \frac{\partial S_{13,0}^2}{\partial \xi_{22}},
$$

where the stress resultant N corresponds to the stiff layers, while the stress resultant T and stress couple G are associated with the soft layer. Introducing the average displacement U and the angle of rotation ϕ as

$$
U = \frac{h_1 u_1 + h_3 u_3}{h_1 + h_3} \approx \frac{h_2(h_1 w_1 + h_3 w_3)}{h_1 + h_3}, \qquad \phi = \frac{u_1 - u_3}{h_2} \approx w_2, \tag{5.33}
$$

we can re-write above equations (5.31) in terms of the integral quantities defined in

(5.32) and (5.33)

$$
\begin{aligned}
\frac{\partial \text{N}}{\partial \text{x}_1} - \rho_1(\text{h}_1 + \text{h}_3)\frac{\partial^2 \text{U}}{\partial \text{t}^2} &= \text{F}_3 - \text{F}_1, \\
\frac{12}{\text{h}_2\mu}\frac{\partial \text{G}}{\partial \text{x}_1} - \left(\frac{1}{\text{h}_1} + \frac{1}{\text{h}_3}\right)\text{T} - \rho_1\text{h}_2^2\frac{\partial^2 \phi}{\partial \text{t}^2} &= -\text{h}_2\left(\frac{\text{F}_3}{\text{h}_3} + \frac{\text{F}_1}{\text{h}_1}\right).
\end{aligned}
\tag{5.34}
$$

The forces T, N and the moment G at leading order can be expressed in terms of U

and ϕ as

$$
\text{T} = \text{h}_2\mu_2\phi,
$$

$$
\text{N} = \mu_1\left(\text{h}_1 + \text{h}_3\right)\frac{\partial \text{U}}{\partial \text{x}_1},
\tag{5.35}
$$

$$
\text{G} = \frac{\mu_2\text{h}_2^3}{12}\frac{\partial \phi}{\partial \text{x}_1}.
$$

Finally, equations (5.34) can be presented as

$$
\begin{aligned}
\mu_1(\text{h}_1 + \text{h}_3)\frac{\partial^2 \text{U}}{\partial \text{x}_1^2} - \rho_1(\text{h}_1 + \text{h}_3)\frac{\partial^2 \text{U}}{\partial \text{t}^2} &= \text{F}_3 - \text{F}_1, \\
\mu_1\text{h}_2\frac{\partial^2 \phi}{\partial \text{x}_1^2} - \mu_2\left(\frac{1}{\text{h}_1} + \frac{1}{\text{h}_3}\right)\phi - \rho_1\text{h}_2\frac{\partial^2 \phi}{\partial \text{t}^2} &= -\left(\frac{\text{F}_3}{\text{h}_3} + \frac{\text{F}_1}{\text{h}_1}\right),
\end{aligned}
\tag{5.36}
$$

governing the sought for two-mode low-frequency model in case of shear stresses,

prescribed at the faces of the considered laminate.

5.4   Asymptotic derivation of boundary conditions

First, consider static equilibrium of a semi-infinite three-layered strip ($0 \leqslant x_1 < +\infty$, $-h_3 - h_2/2 \leqslant x_2 \leqslant h_2/2 + h_1$) with the geometrical and mechanical properties specified in Section 5.1, see Figure 5.1.
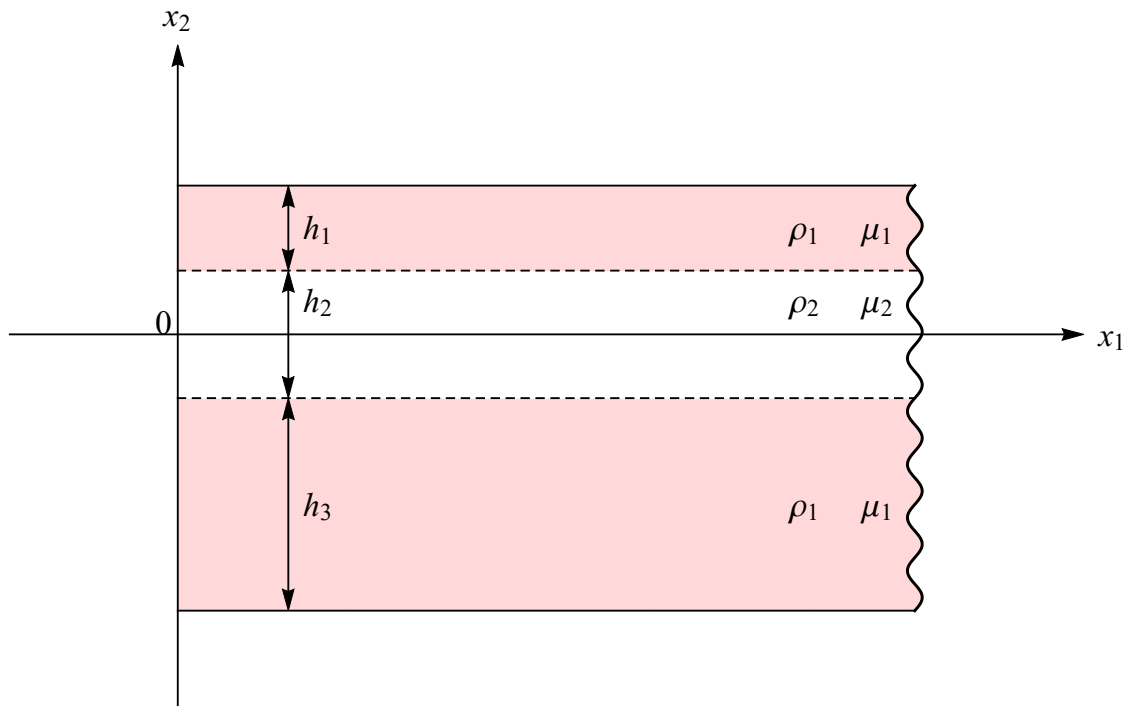
FIGURE 5.1: A semi-infinite three-layered strip

Let the strip faces are traction free, while its left edge $x_1 = 0$ is subject to prescribed stress $p(x_2)$

$$\sigma_{13}^{q}\big|_{x_1=0} = p(x_2), \qquad q = 1, 2, 3. \tag{5.37}$$

Our goal is to find the so-called decay conditions on the function p when

$$\sigma_{13}^{q}\big|_{x_1=+\infty} = 0, \quad q = 1, 2, 3. \tag{5.38}$$

Moreover, we require the related boundary layer to be localised over the narrow vicinity of the edge of width h (h $\sim$ h$_1$ $\sim$ h$_2$ $\sim$ h$_3$), which does not depend on the small contrast parameter μ, defined above. Thus, we assume

$$\frac{\partial}{\partial x_1} \sim \frac{\partial}{\partial x_2} \sim \frac{1}{h}. \tag{5.39}$$

Let us start from the static counterpart of equations (4.1), i.e.

$$\frac{\partial \sigma_{13}^{q}}{\partial x_1} + \frac{\partial \sigma_{23}^{q}}{\partial x_2} = 0, \qquad q = 1, 2, 3, \tag{5.40}$$

subject to homogeneous boundary conditions along the faces (5.1), setting $F_1 = F_3 = 0$ and continuity conditions (4.3), together with (5.37) and (5.38). Integrating the equation of motion for the upper layer (q = 1) over the domain $0 \leqslant x_1 < +\infty$ and $h_2 \leqslant x_2 \leqslant h_2 + h_1$ and applying the aforementioned continuity and boundary

conditions, we obtain

$$
\int_0^{+\infty} \int_{h_2/2}^{h_2/2+h_1} \left(\frac{\partial \sigma_{13}^1}{\partial x_1} + \frac{\partial \sigma_{23}^1}{\partial x_2} \right) dx_2 dx_1 =
$$
$$
\int_{h_2/2}^{h_2/2+h_1} \sigma_{13}^1 \Big|_{x_1=0}^{+\infty} dx_2 + \int_0^{+\infty} \sigma_{23}^1 \Big|_{x_2=h_2/2}^{h_2/2+h_1} dx_1 = \tag{5.41}
$$
$$
- \int_{h_2/2}^{h_2/2+h_1} p(x_2) dx_2 - \int_0^{+\infty} \sigma_{23}^1 \Big|_{x_2=h_2/2} dx_1 = 0.
$$

Hence,

$$
\int_0^{+\infty} \sigma_{23}^1 \Big|_{x_2=h_2/2} dx_1 = - \int_{h_2/2}^{h_2/2+h_1} p(x_2) dx_2 \tag{5.42}
$$

Similarly, for the bottom layer (q = 3) we derive

$$
\int_0^{+\infty} \int_{-h_2/2-h_3}^{-h_2/2} \left(\frac{\partial \sigma_{13}^3}{\partial x_1} + \frac{\partial \sigma_{23}^3}{\partial x_2} \right) dx_2 dx_1 =
$$
$$
- \int_{-h_2/2-h_3}^{-h_2/2} p(x_2) dx_2 + \int_0^{+\infty} \sigma_{23}^3 \Big|_{x_2=-h_2/2} dx_1 = 0. \tag{5.43}
$$

Therefore,

$$
\int_0^{+\infty} \sigma_{23}^3 \Big|_{x_2=-h_2/2} dx_1 = \int_{-h_2/2-h_3}^{-h_2/2} p(x_2) dx_2. \tag{5.44}
$$

For the middle layer (q = 2) we first integrate the associated equation of motion, resulting in

$$\int_0^{+\infty} \int_{-h_2/2}^{h_2/2} \left(\frac{\partial \sigma_{13}^2}{\partial x_1} + \frac{\partial \sigma_{23}^2}{\partial x_2} \right) dx_2 dx_1 =$$

$$- \int_{-h_2/2}^{h_2/2} p(x_2) dx_2 + \int_0^{+\infty} \sigma_{23}^2 \Big|_{x_2=h_2/2} dx_1 - \int_0^{+\infty} \sigma_{23}^2 \Big|_{x_2=-h_2/2} dx_1 = 0. \tag{5.45}$$

Now, we substitute (5.42) and (5.44) into the latter, taking into account the continuity conditions. As might be expected, the following exact result corresponds to the conventional decay condition, expressing the classical formulation of the Saint-Venant principle. It manifests self-equilibrium of the external load and is given by

$$\int_{-h_2/2-h_3}^{h_2/2+h_1} p(x_2) dx_2 = 0. \tag{5.46}$$

Next, we multiply the equation of motion for the middle layer by x_2 and integrate

again over its area. We obtain

$$
\int_0^{+\infty} \int_{-h_2/2}^{h_2/2} x_2 \left(\frac{\partial \sigma_{13}^2}{\partial x_1} + \frac{\partial \sigma_{23}^2}{\partial x_2} \right) dx_2 dx_1 =
$$

$$
\int_{-h_2/2}^{h_2/2} x_2 \sigma_{13}^2 \Big|_{x_1=0}^{+\infty} dx_2 + \int_0^{+\infty} \int_{-h_2/2}^{h_2/2} x_2 \frac{\partial \sigma_{23}^2}{\partial x_2} dx_2 dx_1 =
$$

$$
-\int_{-h_2/2}^{h_2/2} x_2 p(x_2) dx_2 + \int_0^{+\infty} \left(x_2 \sigma_{23}^2 \Big|_{x_2=-h_2/2}^{h_2/2} - \int_{-h_2/2}^{h_2/2} \sigma_{23}^2 dx_2 \right) dx_1 =
$$

$$
-\int_{-h_2/2}^{h_2/2} x_2 p(x_2) dx_2 + \frac{h_2}{2} \int_0^{+\infty} \left(\sigma_{23}^2 \Big|_{x_2=h_2/2} + \sigma_{23}^2 \Big|_{x_2=-h_2/2} \right) dx_1
$$

$$
-\int_0^{+\infty} \int_{-h_2/2}^{h_2/2} \sigma_{23}^2 dx_2 dx_1 \approx
$$

$$
-\int_{-h_2/2}^{h_2/2} x_2 p(x_2) dx_2 + \frac{h_2}{2} \int_0^{+\infty} \left(\sigma_{23}^2 \Big|_{x_2=h_2/2} + \sigma_{23}^2 \Big|_{x_2=-h_2/2} \right) dx_1 = 0,
$$

(5.47)

where we have neglected the asymptotically small $O(\mu)$ term

$$
\int_0^{+\infty} \int_{-h_2/2}^{h_2/2} \sigma_{23}^2 dx_2 dx_1 = \mu_2 \int_0^{+\infty} u_2 \Big|_{x_2=-h_2/2}^{h_2/2} dx_1 \sim \mu.
$$

(5.48)

This is due to the effect of contrast, resulting in a sort of squeezing of the softer

middle layer by the stiff outer layers. In fact, we may readily deduce that in

the last formula $\sigma_{23}^2 \sim p$ while $u_2(x_1, h_2/2) = u_1(x_1, h_2/2) \sim \dfrac{h\sigma_{23}^1}{\mu_1} \sim \dfrac{hp}{\mu_1}$ and

$u_2(x_1, -h_2/2) = u_3(x_1, -h_2/2) \sim \dfrac{h\sigma_{23}^3}{\mu_1} \sim \dfrac{hp}{\mu_1}$. These asymptotic estimates follow

from the aforementioned condition on the boundary layer given by (5.39), which allow to relate the asymptotic orders of stresses and displacements of the thin high contrast strip, also using the continuity conditions. Next, substituting (5.42) and (5.44) into (5.45) we obtain the second decay condition on the prescribed edge load p

$$\int_{-h_2/2}^{h_2/2} x_2 p(x_2) dx_2 + \frac{h_2}{2} \int_{h_2/2}^{h_2/2+h_1} p(x_2) dx_2 - \frac{h_2}{2} \int_{-h_2/2-h_3}^{-h_2/2} p(x_2) dx_2 = 0, \quad (5.49)$$

which is, in contrast with the first "exact" condition (5.46), is of an asymptotic nature and holds only for high contrast laminates. At $h_1 = h_3$ and $p(-x_2) = -p(x_2)$ the last formula reduces to decay conditions (5.78), derived using Laplace transform technique below.

It can be easily shown, see e.g. Babenkova and Kaplunov [2004], that obtained decay conditions (5.46) and (5.49) are also valid at leading order for the low-frequency setup considered in this case $(\partial/\partial t \ll h\sqrt{\rho_k/\mu_k}, \quad k = 1, 2)$.

Let us then adopt the latter for deriving the leading order boundary conditions at the edge $x_1 = 0$ of the laminate governed by formulae (4.1) and (5.1), subject to an

arbitrary low-frequency loading $P(x_2, t)$, i.e.

$$\sigma_{13}^q \big|_{x_1=0} = P(x_2, t), \quad q = 1, 2, 3. \tag{5.50}$$

It is obvious that the function $P(x_2, t)$ is not assumed to satisfy two decay conditions

above in contrast to the function $p(x_2)$.

As usual, see Goldenveizer [1976, 1998], Babenkova and Kaplunov [2003] for greater

detail, insert the discrepancy of the prescribed edge load P and stresses σ_{13}^q, resulting

from the equations of motion established in Section 5.3, into the decay conditions.

Neglecting asymptotically secondary stress σ_{13}^2, see formula (5.4), we set in (5.46)

and (5.49)

$$p = P - \sigma_{13}^1, \qquad\qquad \frac{h_2}{2} < x_2 < \frac{h_2}{2} + h_1, \tag{5.51}$$

$$p = P, \qquad\qquad -\frac{h_2}{2} < x_2 < \frac{h_2}{2}, \tag{5.52}$$

$$p = P - \sigma_{13}^3, \qquad\qquad -h_3 - \frac{h_2}{2} < x_2 < -\frac{h_2}{2}, \tag{5.53}$$

having

$$\int_{h_2/2}^{h_2/2+h_1} (P - \sigma_{13}^1) dx_2 + \int_{-h_2/2}^{h_2/2} P dx_2 + \int_{-h_3-h_2/2}^{-h_2/2} (P - \sigma_{13}^3) dx_2 = 0, \tag{5.54}$$

and

$$\int_{-h_2/2}^{h_2/2} x_2 P dx_2 + \frac{h_2}{2} \int_{h_2/2}^{h_2/2+h_1} (P - \sigma_{13}^1) dx_2 - \frac{h_2}{2} \int_{-h_2/2-h_3}^{-h_2/2} (P - \sigma_{13}^3) dx_2 = 0, \quad (5.55)$$

Finally, expressing σ_{13}^1 and σ_{13}^3 in (5.54) through N by formulae (5.32), first boundary condition becomes

$$N = \int_{-h_3-h_2/2}^{h_2/2+h_1} P dx_2. \quad (5.56)$$

Similarly, expressing second condition (5.55) through N and G and using the last equation, we obtain

$$\int_{-h_2/2}^{h_2/2} x_2 P dx_2 + \frac{h_2}{2} \int_{h_2/2}^{h_2/2+h_1} P dx_2 - \frac{h_2}{2} \int_{-h_2/2-h_3}^{-h_2/2} P dx_2$$
$$+ \frac{h_2}{2} \left(\frac{h_1 - h_3}{h_1 + h_3} N + \frac{24 h_1 h_3}{\mu h_2^2 (h_1 + h_3)} G \right) = 0, \quad (5.57)$$

resulting in

$$G = -\frac{\mu h_2 (h_1 + h_3)}{12 h_1 h_3} \left(\int_{-h_2/2}^{h_2/2} x_2 P dx_2 + \frac{h_2}{2} \int_{h_2/2}^{h_2/2+h_1} P dx_2 \right.$$
$$\left. - \frac{h_2}{2} \int_{-h_2/2-h_3}^{-h_2/2} P dx_2 + \frac{h_2}{2} \frac{h_1 - h_3}{h_1 + h_3} \int_{-h_2/2-h_3}^{h_2/2+h_1} P dx_2 \right). \quad (5.58)$$

Derived boundary conditions (5.56) and (5.58) correspond to the first and second equations in (5.34), respectively. They can be also expressed through the average

displacement U and the angle of rotation ϕ using (5.35)

$$\frac{\partial U}{\partial x_1} = \frac{1}{\mu_1 (h_1 + h_3)} \int_{-h_3-h_2/2}^{h_2/2+h_1} P dx_2,$$

$$\frac{\partial \phi}{\partial x_1} = -\frac{(h_1 + h_3)}{h_1 h_2^2 h_3 \mu_1} \left(\int_{-h_2/2}^{h_2/2} x_2 P dx_2 + \frac{h_2}{2} \int_{h_2/2}^{h_2/2+h_1} P dx_2 \right.$$

$$\left. - \frac{h_2}{2} \int_{-h_2/2-h_3}^{-h_2/2} P dx_2 + \frac{h_2}{2} \frac{h_1 - h_3}{h_1 + h_3} \int_{-h_2/2-h_3}^{h_2/2+h_1} P dx_2 \right).$$

It is obvious that the boundary conditions above can be also imposed at each of the edges of a finite length thin strip. In the latter case, an extra exponentially small error will naturally arise, along with standard observations typical for thin elastic structures, e.g. see Goldenveizer [1976].

5.5 Laplace transform technique for a symmetric plate

Let us now establish the decay conditions for a symmetric three-layered plate ($h_1 = h_3$) with traction free faces using Laplace transform technique. We restrict ourselves with the motion for which the displacements of the laminate are odd functions in x_2, i.e. $u_2(x_1, -x_2) = -u_2(x_1, x_2)$, $u_3(x_1, -x_2) = u_1(x_1, x_2)$.

Let the functions $U_q(s, x_2)$ denote Laplace transform of displacements u_q, $q = 1, 2, 3$,

i.e.

$$U_q(s, x_2) = \int_0^\infty u_q(x_1, x_2) e^{-sx_1} dx_1, \tag{5.59}$$

where s is Laplace transform parameter. Transforming equilibrium equations (5.40),

we get

$$\frac{\partial^2 U_q}{\partial x_2^2} + s^2 U_q = R_q, \tag{5.60}$$

where $R_q(s, x_2)$ are defined through

$$R_q(s, x_2) = s u_q \big|_{x_1=0} + \frac{\partial u_q}{\partial x_1}\bigg|_{x_1=0} = s u_q \big|_{x_1=0} + \frac{p(x_2)}{\mu_q}. \tag{5.61}$$

Solving equations (5.60) for the odd displacements, we have

$$U_1 = A_1(s) \sin sx_2 + A_2(s) \cos sx_2 + \frac{1}{s} \int_0^{x_2} R_1(s, x_2') \sin s(x_2 - x_2') dx_2', \tag{5.62}$$

and

$$U_2 = B_1(s) \sin sx_2 + \frac{1}{s} \int_0^{x_2} R_2(s, x_2') \sin s(x_2 - x_2') dx_2', \tag{5.63}$$

where unknown functions A_1, A_2 and B_1 are determined from the transformed bound-

ary and continuity conditions and given by

$$
\begin{aligned}
A_1(s) = D^{-1}(s)\Big\{ &- C_1\left(h_1 + \frac{h_2}{2}\right)\left(\mu\cos^2\frac{sh_2}{2} + \sin^2\frac{sh_2}{2}\right) \\
&+ \left(S_2\left(\frac{h_2}{2}\right) - S_1\left(\frac{h_2}{2}\right)\right)\mu\sin\left(sh_1 + \frac{sh_2}{2}\right)\cos\frac{sh_2}{2} \\
&+ \left(C_1\left(\frac{h_2}{2}\right) - \mu C_2\left(\frac{h_2}{2}\right)\right)\sin\left(sh_1 + \frac{sh_2}{2}\right)\sin\frac{sh_2}{2}\Big\},
\end{aligned}
$$
(5.64)

$$
\begin{aligned}
A_2(s) = D^{-1}(s)\Big\{ &C_1\left(h_1 + \frac{h_2}{2}\right)(\mu - 1)\sin\frac{sh_2}{2}\cos\frac{sh_2}{2} \\
&+ \left(S_2\left(\frac{h_2}{2}\right) - S_1\left(\frac{h_2}{2}\right)\right)\mu\cos\left(sh_1 + \frac{sh_2}{2}\right)\cos\frac{sh_2}{2} \\
&+ \left(C_1\left(\frac{h_2}{2}\right) - \mu C_2\left(\frac{h_2}{2}\right)\right)\cos\left(sh_1 + \frac{sh_2}{2}\right)\sin\frac{sh_2}{2}\Big\},
\end{aligned}
$$
(5.65)

and

$$
\begin{aligned}
B_1(s) = D^{-1}(s)\Big\{ &- C_1\left(h_1 + \frac{h_2}{2}\right) + \left(S_2\left(\frac{h_2}{2}\right) - S_1\left(\frac{h_2}{2}\right)\right)\sin sh_1 \\
&+ \left(C_1\left(\frac{h_2}{2}\right) - \mu C_2\left(\frac{h_2}{2}\right)\right)\cos sh_1\Big\},
\end{aligned}
$$
(5.66)

where

$$
D(s) = s\left(\mu\cos sh_1\cos\frac{sh_2}{2} - \sin sh_1\sin\frac{sh_2}{2}\right),
$$
(5.67)

and

$$
C_q(s, x_2) = \int_0^{x_2} R_q(x_2')\cos s(x_2 - x_2')dx_2',
$$
(5.68)

$$S_q(s, x_2) = \int_0^{x_2} R_q(x_2') \sin s(x_2 - x_2') dx_2', \quad q = 1, 2. \tag{5.69}$$

The sought for displacements are expressed through Mellin integrals as

$$u_q(x_1, x_2) = \frac{1}{2\pi i} \int_{\delta-i\infty}^{\delta+i\infty} U(s, x_2) e^{sx_1} ds \tag{5.70}$$

for $\delta > 0$. These integrals can be found using the residue theory

$$u_q(x_1, x_2) = \sum_{n=0}^{\infty} \text{Res}_{s_n}\{U_q(s, x_2) e^{sx_1}\}, \tag{5.71}$$

where only small poles s_n, corresponding to unwanted slow decay are of the concern, see also Gusein-Zade [1965], Babenkova and Kaplunov [2004].

At $\mu \ll 1$ and $s \ll 1$ the leading order asymptotic behaviour of denominator (5.67) is given by

$$D(s) = -2s(h_1 h_2 s^2 - \mu), \tag{5.72}$$

resulting in two small non-zero roots

$$s^{\pm} = \pm\sqrt{\frac{2\mu}{h_1 h_2}}. \tag{5.73}$$

The associated residues are

$$\text{Res}_{s\pm} \left\{ U_1(s,x_2)e^{sx_1} \right\} = \text{Res}_{s\pm} \left\{ D^{-1}(s) \left(A_1(s) \sin sx_2 + A_2(s) \cos sx_2 \right) e^{sx_1} \right\},$$

$$\text{Res}_{s\pm} \left\{ U_2(s,x_2)e^{sx_1} \right\} = \text{Res}_{s\pm} \left\{ D^{-1}(s) B_1(s) \sin sx_2 e^{sx_1} \right\},$$

$$(5.74)$$

where $D(s)$ is defined in (5.72).

Expanding now the numerators in these relations at $\mu \ll 1$ and $s \sim \sqrt{\mu}$ and using the formula

$$R_2 = su_2\big|_{x_1=0} + \frac{p(x_2)}{\mu\mu_1}, \qquad (5.75)$$

we obtain at leading order

$$\text{Res}_{s\pm} = \pm \frac{\sqrt{2h_2}}{4\mu_1\sqrt{h_1}\sqrt{\mu}} \left(\int_{h_2/2}^{h_2/2+h_1} p(x_2)dx_2 + \frac{2}{h_2} \int_0^{h_2/2} p(x_2)x_2 dx_2 \right), \qquad (5.76)$$

and

$$\text{Res}_{s\pm} = \pm \frac{\sqrt{2}x_2}{2\mu_1\sqrt{h_1h_2}\sqrt{\mu}} \left(\int_{h_2/2}^{h_2/2+h_1} p(x_2)dx_2 + \frac{2}{h_2} \int_0^{h_2/2} p(x_2)x_2 dx_2 \right), \qquad (5.77)$$

for u_1 and u_2, respectively.

These residues diminish at

$$\int_{h_2/2}^{h_2/2+h_1} p(x_2)dx_2 + \frac{2}{h_2}\int_0^{h_2/2} p(x_2)x_2dx_2 = 0, \qquad (5.78)$$

ensuring strong decay of the boundary layer. The latter equation can be restored

from a more general one (5.49), obtained in the previous section, by taking $p(x_2)$ in

(5.49) to be an odd function, i.e. $p(-x_2) = -p(x_2)$.

5.6   Concluding remarks

The consideration in the chapter is seemingly the optimal scalar boundary value problem for elucidating the effect of high contrast. In spite to asymmetry of the plate, the leading order equations of motion are not coupled. The findings in the chapter facilitate asymptotic analysis of various more sophisticated formulations for strongly inhomogeneous thin structures, including vector problems for multi-layered laminates with a variety of contrast setups.

A weak boundary layer, noted earlier in statics of high-contrast laminates, e.g. see Horgan [1998], can be naturally embedded into the low-dimensional theory for the interior domain, see 1D equation (5.31). This is in line with the observation that the lowest harmonic describes both static (and quasi-static) slow decay and near cut-off long wave propagation.

Asymptotically consistent boundary conditions (5.56) and (5.58) are established using the Saint-Venant principle adapted for a high-contrast plate. It is remarkable that the extra approximate decay condition (5.49) is not directly related to the overall equilibrium as the traditional exact decay condition (5.46).

Chapter 6

Two-mode non-uniform approximations for a three-layered plate

An elastic asymmetric sandwich is considered under the assumption that the stiffness and density of thin skin layers are much greater than those of a core layer. As above, it is shown that for typical values of problem parameters the lowest shear resonance frequency appears to be asymptotically small, while the rest of thickness resonances do not belong to a low-frequency range. The same as in Chapters 2-5

99

scalar antiplane problem in linear elasticity is studied.

A polynomial long-wave low-frequency approximation of the full dispersion relation is derived. Again, it governs two vibration modes including the fundamental one and the lowest harmonic. It is obvious that without asymmetry the dispersion relation splits into two parts corresponding to symmetric and antisymmetric modes Prikazchikova et al. [2020], simplifying analysis drastically. It is remarkable that for the chosen set of problem parameters the derived approximation is not asymptotically uniform and is only valid over narrow non-overlapping vicinities of zero and the lowest shear thickness resonance frequencies.

This is in contrast to the setup of a similar laminate with the thick skin layers, for which the associated asymptotic behaviour is uniform, see Chapters 4-5. The same observation is also true for in-plane motion of a symmetric laminate, see Kaplunov et al. [2017a] for further detail.

6.1   Dispersion analysis

Consider a three-layered asymmetric elastic laminate, comprised of isotropic layers of thickness h_q, $q = 1, 2, 3$, see Figure 6.1. Let us assume in this chapter that the outer layers are thin in comparison to the core one, i.e. $h_1 \ll h_2$ and $h_3 \ll h_2$, while $h_1 \sim h_3$. As before, we assume that the two outer layers have the same material parameters.
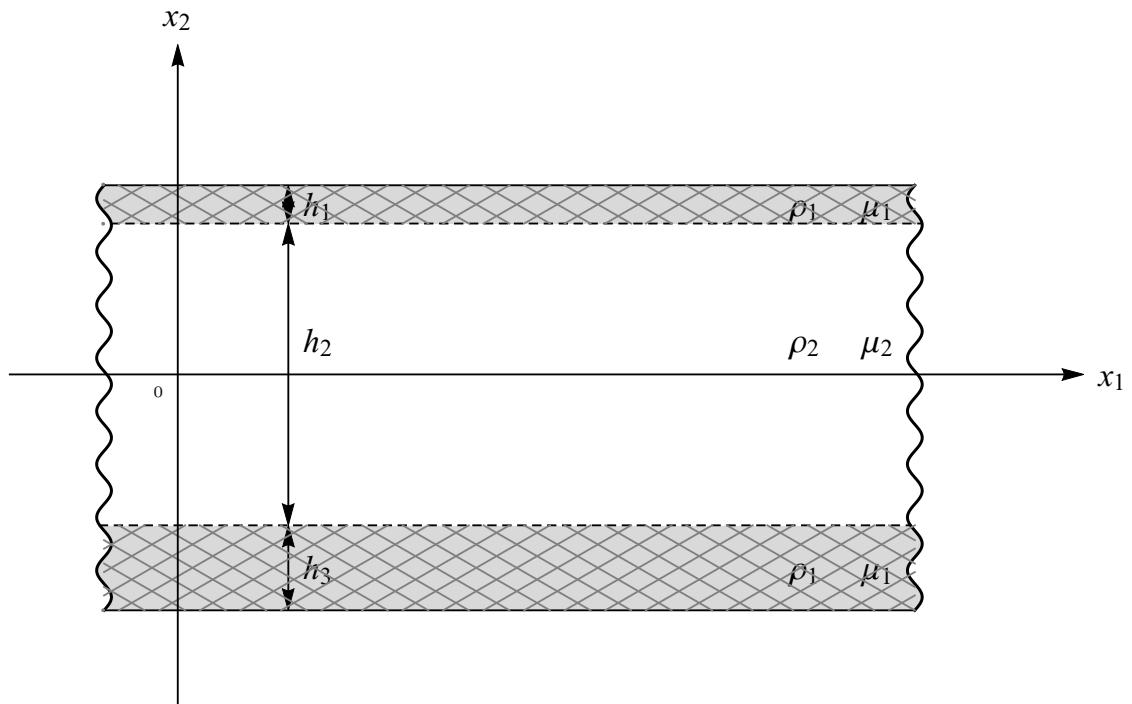
FIGURE 6.1: A three-layered asymmetric laminate with thin outer layers

We start from the dispersion relation (4.12), with the focus on the high contrast setup for which

$$\mu \ll 1, \quad \rho \sim \mu^2, \quad h_{12} \sim \mu, \quad h_{32} \sim \mu. \tag{6.1}$$

This formulae correspond to an asymmetric laminate of a sandwich type, with the outer layers being stiff, thin and very heavy compared to the inner core layer.

In this case the lowest shear cut-off frequency is also defined by the asymptotic estimate (4.23) and is O($\sqrt{\mu}$) as above. At the same time, now, in view of (6.1), leading order coefficients γ_i in the polynomial dispersion relation (4.24) become

$$\gamma_1 = \gamma_1^0 \mu^2, \qquad \gamma_1^0 = 1 + h_{12}^0 + h_{32}^0,$$

$$\gamma_2 = \gamma_2^0 \mu + O\left(\mu^2\right), \qquad \gamma_2^0 = -\frac{h_{12}^0 + h_{32}^0}{\rho_0},$$

$$\gamma_3 = \gamma_3^0 \mu^2 + O\left(\mu^4\right), \qquad \gamma_3^0 = h_{12}^0 h_{32}^0 - \frac{1}{3},$$

$$\gamma_4 = \gamma_4^0 \mu + O\left(\mu^2\right), \qquad \gamma_4^0 = -\frac{2h_{12}^0 h_{32}^0}{\rho_0},$$

$$\gamma_5 = \gamma_5^0 + O\left(\mu^2\right), \qquad \gamma_5^0 = \frac{h_{12}^0 h_{32}^0}{\rho_0^2}, \tag{6.2}$$

$$\gamma_6 = \gamma_6^0 \mu^2 + O\left(\mu^4\right), \qquad \gamma_6^0 = \frac{2}{15} - \frac{h_{12}^0 h_{32}^0}{3},$$

$$\gamma_7 = \gamma_7^0 \mu + O\left(\mu^2\right), \qquad \gamma_7^0 = \frac{2h_{12}^0 h_{32}^0}{3\rho_0},$$

$$\gamma_8 = \gamma_8^0 + O\left(\mu\right), \qquad \gamma_8^0 = -\frac{h_{12}^0 h_{32}^0}{3\rho_0^2},$$

$$\gamma_9 = \gamma_9^0 + O\left(\mu\right), \qquad \gamma_9^0 = \frac{h_{12}^0 h_{32}^0}{3\rho_0^2},$$

where $\rho_0 = \rho/\mu^2$, $h_{12}^0 = h_{12}/\mu$ and $h_{32}^0 = h_{32}/\mu$. These results are summarised in Table 6.1, allowing comparison of asymptotic orders of the terms in approximation

(4.24) both in the vicinity of zero and the lowest cut-off frequency (4.23).

Order of γ_i	Terms	Fundamental mode $\Omega^2 \sim \mu K^2$	First harmonic $\Omega_{sh}^2 \sim \mu$
$\gamma_1 \sim \mu^2$	$\gamma_1 K^2$	$\mu^2 K^2$	$\mu^2 K^2$
$\gamma_2 \sim \mu$	$\gamma_2 \Omega^2$	$\mu^2 K^2$	μ^2
$\gamma_3 \sim \mu^2$	$\gamma_3 K^4$	$\mu^2 K^4$	$\mu^2 K^4$
$\gamma_4 \sim \mu$	$\gamma_4 K^2 \Omega^2$	$\mu^2 K^4$	$\mu^2 K^2$
$\gamma_5 \sim 1$	$\gamma_5 \Omega^4$	$\mu^2 K^4$	μ^2
$\gamma_6 \sim \mu^2$	$\gamma_6 K^6$	$\mu^2 K^6$	$\mu^2 K^6$
$\gamma_7 \sim \mu$	$\gamma_7 K^4 \Omega^2$	$\mu^2 K^6$	$\mu^2 K^4$
$\gamma_8 \sim 1$	$\gamma_8 K^2 \Omega^4$	$\mu^2 K^6$	$\mu^2 K^2$
$\gamma_9 \sim 1$	$\gamma_9 \Omega^6$	$\mu^3 K^6$	μ^3

TABLE 6.1: Asymptotic behaviour at $\mu \ll 1, \quad \rho \sim \mu^2, \quad h_{12} \sim h_{32} \sim \mu$

6.2   Two-mode shortened dispersion relation

Using the Table 6.1, the leading order shortened approximate dispersion relation may

be constructed, incorporating the fundamental mode along with the lowest harmonic

with the asymptotically small cut-off frequency (4.23). It may be expressed as

$$\mu^2 \gamma_1^0 K^2 + \left(\mu \gamma_2^0 + \gamma_5^0 \Omega^2 \right) \Omega^2 + \mu \gamma_4^0 K^2 \Omega^2 + \gamma_8^0 K^2 \Omega^4 + \gamma_9^0 \Omega^6 = 0. \qquad (6.3)$$

In this formula all the terms are of the same order μ^3 at $\Omega - \Omega_{\mathrm{sh}} \sim \mu^{3/2}$, $K \sim \sqrt{\mu}$.

The local asymptotic approximation for the fundamental mode is given by

$$\mu \gamma_1^0 K^2 + \gamma_2^0 \Omega^2 = 0. \qquad (6.4)$$

At the same time, the local expansion for the first harmonic becomes

$$\mu^2 \gamma_1^0 K^2 + \left(\mu \gamma_2^0 + \gamma_5^0 \Omega^2 \right) \Omega^2 + \mu \gamma_4^0 K^2 \Omega^2 + \gamma_8^0 K^2 \Omega^4 + \gamma_9^0 \Omega^6 = 0. \qquad (6.5)$$

The associated local near cut-off expansion, e.g. see Kaplunov and Markushevich

[1993], Lashhab et al. [2015] for further details, is

$$\Omega^2 - \Omega_{\text{sh}}^2 = -\text{K}^2 \frac{1}{\gamma_5^0} \left(\mu^2 \frac{\gamma_1^0}{\Omega_{\text{sh}}^2} + \mu \gamma_4^0 + \gamma_8^0 \Omega_{\text{sh}}^2 \right) - \frac{\gamma_9^0 \Omega_{\text{sh}}^4}{\gamma_5^0} \qquad (6.6)$$

where Ω_{sh} is given by (4.23).

Note that the long-wave assumption $\text{K} \ll 1$ dictates that the approximation (6.4)

for the fundamental mode is valid only for $\Omega \ll \sqrt{\mu}$, whereas (6.6) is associated

with $\Omega \sim \sqrt{\mu}$. Thus, the approximation (6.3) is non-uniform, in line with previous

considerations in Kaplunov et al. [2017a,b].

Numerical illustrations of the derived approximations are given in Figures 6.2-6.4.

In Figure 6.2 two-mode approximation (6.3) (dotted lines) is compared numerically

with the exact solution of the dispersion relation (4.12) (solid lines). A characteristic

gap where the asymptotic formula (6.3) is not applicable is shown in Figure 6.2.
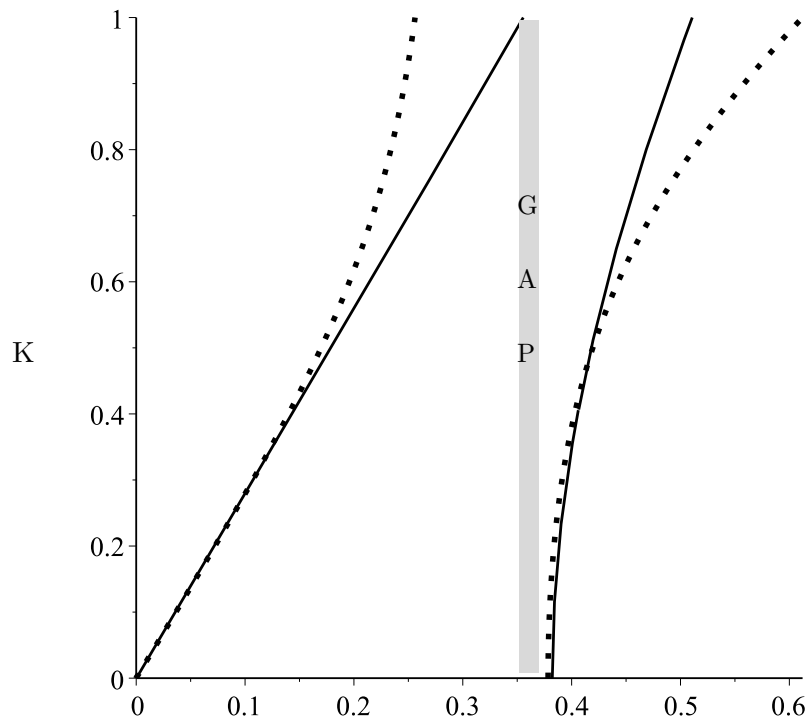
FIGURE 6.2: Dispersion curves (4.12) (solid lines) together with approximation (6.3) (dotted lines) for $h_{12} = 0.1$, $h_{32} = 0.2$, $\mu = 0.1$, and $\rho = 0.01$.

In Figure 6.2 exact dispersion curves (4.12) (solid lines) are shown together with approximations for the fundamental mode (6.4) and for the lowest harmonic (6.6) (dotted lines), demonstrating high accuracy of asymptotic predictions.

Next two figures present the results of comparison separately for two considered modes, using the local approximations (6.4) and (6.6).
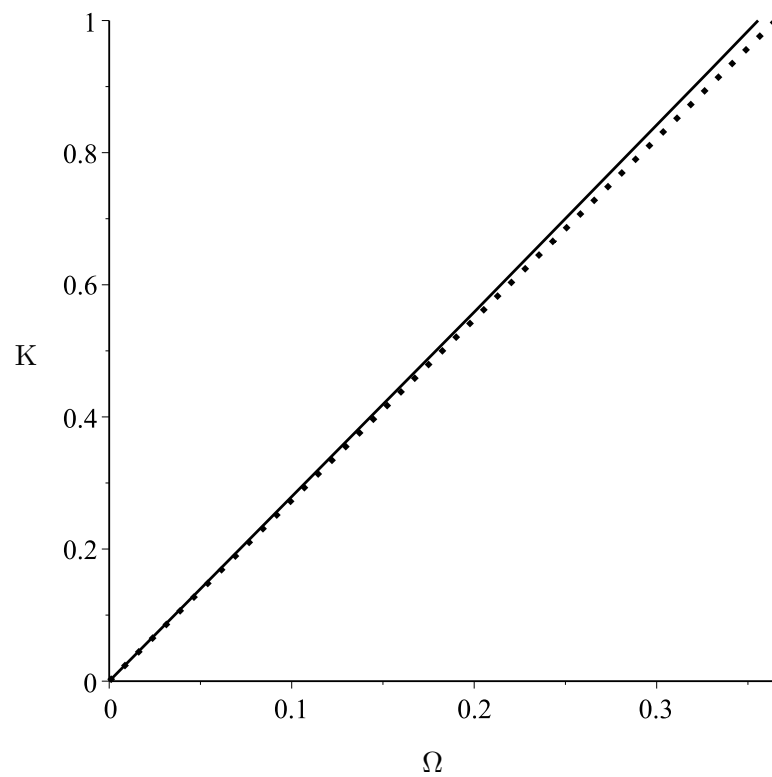
FIGURE 6.3: Dispersion curves (4.12) (solid lines) together with approximations for the fundamental mode (6.4) (dotted lines) for $h_{12} = 0.1$, $h_{32} = 0.2$, $\mu = 0.1$ and $\rho = 0.01$
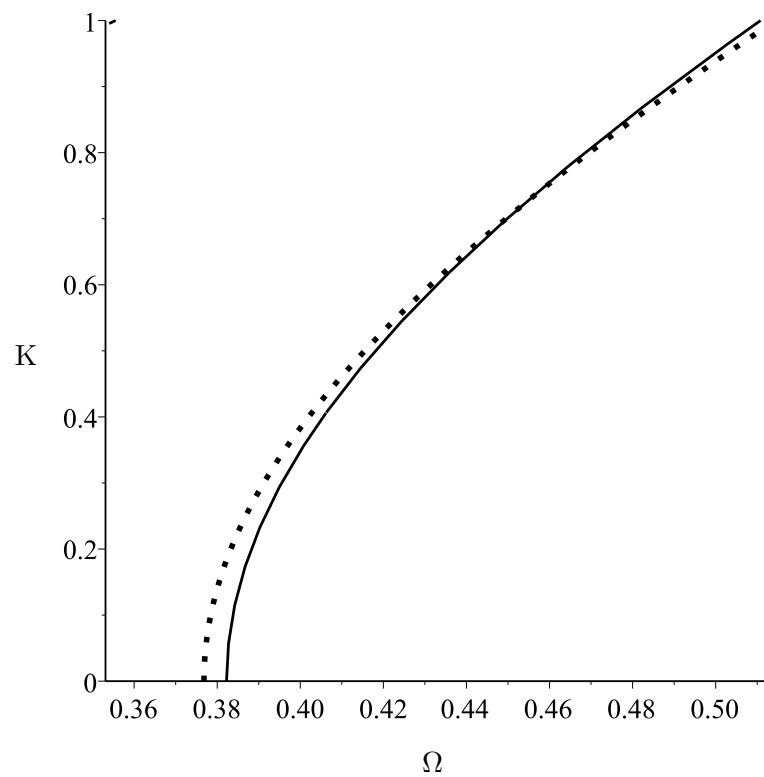
FIGURE 6.4: Dispersion curves (4.12) (solid lines) together with approximations for the lowest harmonic (6.6) (dotted lines) for $h_{12} = 0.1$, $h_{32} = 0.2$, $\mu = 0.1$ and $\rho = 0.01$

6.3   Concluding remarks

The present analysis complements the previous results for an asymmetric layered plate in the previous Chapters 3-4. Two-mode approximate dispersion relation has been derived for the scenario in which the outer layers are relatively stiff, thin and very heavy compared to the inner layer. In contrast to the dispersion analysis in chapter 3, where the two-mode long-wave low-frequency approximation was asymptotically uniform, the approximation obtained in this chapter is of composite nature, being only valid over non-overlapping vicinities of the origin and the first cut-off frequency. Thus, the effect of high contrast does not always result in a uniform two-mode approximation as might be expected. This observation may be expanded to the derivation of the related two-mode differential equations of motion, based on the same scaling similarly to the Chapter 4.

Chapter 7

Conclusions

It is demonstrated that for two-layered laminate the first shear cut-off frequency is small for a high contrast in stiffnesses (and densities) of the layers. In this case the thicknesses of the layers are assumed to be of the same order. The approximate dispersion relations along with associated scalar 1D equations of motion are derived for long-wave low-frequency out of plane vibrations. A good agreement with the numerical implementation of the exact dispersion relation is demonstrated.

For the same as above high contrast scenario, an asymmetric three-layered laminate supports two low-frequency vibration modes, including the fundamental one and the first shear harmonic. A shortened polynomial dispersion equation is derived

for these two modes. This equation is uniformly valid over the range containing the first shear cut-off frequency. Numerical comparison with the solutions of the exact dispersion relation for asymmetric three-layered laminate demonstrates a high accuracy of the developed two-mode shortened relation. The obtained asymptotic results can be extended to various types of high contrast structures, as well as to Lamb-type waves, arising in 2D plane and 3D vector problems in dynamic elasticity for multi-layered plates. They also make an important preliminary insight for the derivation of approximate equations of motion starting from original 2D equations for antiplane shear.

The 1D equation of motion corresponding to the two-mode uniformly valid dispersion relation above are obtained. They are presented both in terms of displacements of the layers as well as through stress resultants and stress couples, average laminate displacement and angle of rotation. External loading is taken into consideration both for loads applied to the faces and the edges of the laminate. For the latter, asymptotically consistent boundary conditions are derived based on the Saint-Venant's principle adapted for the laminate with the chosen contrast properties.

Two-mode approximate dispersion relations are also derived for the scenario in which the outer layers are relatively stiff, thin and very heavy compared to the inner layer. In contrast to the above mentioned set of parameters, in which the two-mode long-wave

low-frequency approximation is asymptotically uniform, the shortened dispersion relation in the considered case is not uniform and is only valid over non-overlapping vicinities of the zero and the first shear cut-off frequencies. Thus, the high contrast is not always lead to a uniform two-mode approximation as might be initially expected. The related differential equations of motion can be also established for this type of contrast.

We also remark that, the transition from uniform to non-uniform asymptotic behaviours occurs in modelling of light-weighted sandwiches, when the relative density of the light filler may vary over a certain parametric range, see Kaplunov et al. [2019a]. The technique presented in this thesis seems to be relevant for further development of the results in the cited paper. This may contribute to the follow-up program.

The immediate follow-up research may be aimed at the derivation of approximate equations of motion and boundary conditions corresponding to the obtained two-mode non-uniform approximation for an elastic asymmetric sandwich. The next step may be oriented to multi-layered plates with various configurations of stiff and soft layers as well as non-ideal interfacial conditions. It is no doubt that the developed methodology can be also extended to a broad range of the dynamic problems outside the studied scalar setup of antiplane shear. At the same time, the problems for

thin-layered shells can be initially tackled, namely within the framework of antiplane

shear.

Bibliography

F. Abramovici and Z. Alterman. Computations pertaining to the problem of propagation of a seismic pulse in a layered solid. *Methods of Computational Physics*, 4: 349–379, 1965.

J. Achenbach. *Wave propagation in elastic solids*. Elsevier, 2012.

L. A. Aghalovyan. *Asymptotic theory of anisotropic plates and shells*. World Scientific, 2015.

L. Ainola and U. Nigul. Wave processes of deformation of elastic plates and shells. *Izvestiya Akademii Nauk Estonskoi SSR, Ser. Fiz.-Mat. Tekhn. Nauk*, 14(1):3–63, 1965.

O. Aksentian and I. Vorovich. The state of stress in a thin plate. *Journal of Applied Mathematics and Mechanics*, 27(6):1621–1643, 1963.

M. Alkinidri, J. Kaplunov, and L. Prikazchikova. Two-mode long-wave low-frequency approximations for anti-plane shear deformation of a high-contrast asymmetric laminate. *Springer Proceedings in Mathematics and Statistics*, DSTA 2019:in press, 2019.

M. Alkinidri, J. Kaplunov, and L. Prikazchikova. A two mode non-uniform approximation for an elastic asymmetric sandwich. In *EURODYN 2020, XI International Conference of Structural Dynamics*, pages 528–535, 01 2020. doi: 10.47964/1120.9041.19171.

I. V. Andrianov, J. Awrejcewicz, and L. I. Manevitch. *Asymptotical mechanics of thin-walled structures.* Springer Science & Business Media, 2013.

J. Arbaoui, Y. Schmitt, J.-L. Pierrot, and F.-X. Royer. Comparison study and mechanical characterisation of a several composite sandwich structures. *International Journal of Composite Materials*, 5(1):1–8, 2015.

M. Z. Aşık and S. Tezcan. A mathematical model for the behavior of laminated glass beams. *Computers & Structures*, 83(21-22):1742–1753, 2005.

E. Babenkova and J. Kaplunov. The two-term interior asymptotic expansion in the case of low-frequency longitudinal vibrations of an elongated elastic rectangle. In

IUTAM Symposium on Asymptotics, Singularities and Homogenisation in Problems of Mechanics, pages 137–145. Springer, 2003.

E. Babenkova and J. Kaplunov. Low–frequency decay conditions for a semi–infinite elastic strip. *Proceedings of the Royal Society of London. Series A: Mathematical, Physical and Engineering Sciences*, 460(2048):2153–2169, 2004.

E. Babenkova and J. Kaplunov. Radiation conditions for a semi-infinite elastic strip. *Proceedings of the Royal Society A: Mathematical, Physical and Engineering Sciences*, 461(2056):1163–1179, 2005.

E. R. Baylis and W. Green. Flexural waves in fibre-reinforced laminated plates. *Journal of Sound and Vibration*, 110(1):1–26, 1986a.

E. R. Baylis and W. Green. Flexural waves in fibre-reinforced laminated plates, part ii. *Journal of Sound and Vibration*, 111(2):181–190, 1986b.

B. Beral. Airbus structure and technology–next steps and vision. In *Proceedings of 16th International Conference on Composite Materials. Kyoto*, 2007.

V. Berdichevskii. High-frequency long-wave vibrations of plates. *Soviet Physics Doklady*, 22:604, 1977.

V. Berdichevskii. Variational-asymptotic method of constructing a theory of shells. *Journal of Applied Mathematics and Mechanics*, 43(4):711–736, 1979.

V. Berdichevskii and L. Starosel'skii. On the theory of curvilinear Timoshenko-type rods. *Journal of Applied Mathematics and Mechanics*, 47(6):809–817, 1983.

V. Berdichevsky. *Variational principles of continuum mechanics: II. Applications.* Springer-Verlag., 2009.

V. L. Berdichevsky. An asymptotic theory of sandwich plates. *International Journal of Engineering Science*, 48(3):383–404, 2010.

V. Beresin, L. Y. Kossovich, and J. Kaplunov. Synthesis of the dispersion curves for a cylindrical shell on the basis of approximate theories. *Journal of Sound and Vibration*, 186(1):37–53, 1995.

C. Boutin and K. Viverge. Generalized plate model for highly contrasted laminates. *European Journal of Mechanics-A/Solids*, 55:149–166, 2016.

C. Chapman. An asymptotic decoupling method for waves in layered media. *Proceedings of the Royal Society A: Mathematical, Physical and Engineering Sciences*, 469(2153):20120659, 2013.

R. Chebakov, J. Kaplunov, and G. Rogerson. Refined boundary conditions on the free surface of an elastic half-space taking into account non-local effects. *Proceedings of the Royal Society A: Mathematical, Physical and Engineering Sciences*, 472(2186): 20150800, 2016.

S. Cheng. On the theory of bending of sandwich plates. *University of Wisconsin–Madison Mathematics Research Center*, 1961.

D. J. Colquitt, V. V. Danishevskyy, and J. Kaplunov. Composite dynamic models for periodically heterogeneous media. *Mathematics and Mechanics of Solids*, 24 (9):2663–2693, 2019.

R. Craster, L. Joseph, and J. Kaplunov. Long-wave asymptotic theories: the connection between functionally graded waveguides and periodic media. *Wave Motion*, 51(4):581–588, 2014.

H.-H. Dai, J. Kaplunov, and D. Prikazchikov. A long-wave model for the surface elastic wave in a coated half-space. *Proceedings of the Royal Society A: Mathematical, Physical and Engineering Sciences*, 466(2122):3097–3116, 2010.

S. Dutton, D. Kelly, and A. Baker. *Composite materials for aircraft structures.* American Institute of Aeronautics and Astronautics, 2004.

I. Elishakoff, J. Kaplunov, and E. Nolde. Celebrating the centenary of Timoshenko's study of effects of shear deformation and rotary inertia. *Applied Mechanics Reviews*, 67(6), 2015.

B. Erbaş, J. Kaplunov, A. Nobili, and G. Kılıç. Dispersion of elastic waves in a layer interacting with a Winkler foundation. *The Journal of the Acoustical Society of America*, 144(5):2918–2925, 2018a.

B. Erbaş, J. Kaplunov, E. Nolde, and M. Palsü. Composite wave models for elastic plates. *Proceedings of the Royal Society A: Mathematical, Physical and Engineering Sciences*, 474(2214):20180103, 2018b.

B. Erbaş, J. Kaplunov, and M. Palsü. A composite hyperbolic equation for plate extension. *Mechanics Research Communications*, 99:64–67, 2019.

A. C. Eringen. Bending and buckling of rectangular sandwich plates. *Journal of Applied Mechanics-Transactions of the ASME*, 18(3):330–330, 1951.

W. M. Ewing, W. S. Jardetzky, F. Press, and A. Beiser. Elastic waves in layered media. *Physics Today*, 10:27, 1957.

K. Friedrichs and R. Dressler. A boundary-layer theory for elastic plates. *Communications on Pure and Applied Mathematics*, 14(1):1–33, 1961.

A. Goldenveizer. The principles of reducing three-dimensional problems of elasticity to two-dimensional problems of the theory of plates and shells. In *Applied Mechanics*, pages 306–311. Springer, 1966.

A. Goldenveizer. *Theory of thin elastic shells (in Russian)*. Izdatel'stvo Nauka, 1976.

A. Goldenveizer. Asymptotic method in the theory of shells. *Theoretical and Applied Mechanics*, pages 91–104, 1980.

A. Goldenveizer. The boundary conditions in the two-dimensional theory of shells. the mathematical aspect of the problem. *Journal of Applied Mathematics and Mechanics*, 62(4):617–629, 1998.

A. Goldenveizer, J. Kaplunov, and E. Nolde. On Timoshenko-Reissner type theories of plates and shells. *International Journal of Solids and Structures*, 30(5):675–694, 1993.

A. L. Goldenveizer. *Theory of Elastic Thin Shells: Solid and Structural Mechanics*, volume 2. Elsevier, 2014.

R. Gregory and F. Wan. On plate theories and Saint-Venant's principle. *International Journal of Solids and Structures*, 21(10):1005–1024, 1985.

R. D. Gregory and F. Y. Wan. Decaying states of plane strain in a semi-infinite strip and boundary conditions for plate theory. *Journal of Elasticity*, 14(1):27–64, 1984.

D. Gridin, R. V. Craster, and A. T. Adamou. Correction for gridin et al., trapped modes in curved elastic plates. *Proceedings of the Royal Society A: Mathematical, Physical and Engineering Sciences*, 461(2064):4057–4061, 2005.

É. Grigolyuk and I. Selezov. Nonclassical theory of vibration of rods, plates, and shells. *Reviews of the Science and Technology*, 5, 1973.

M. Gusein-Zade. On necessary and sufficient conditions for the existence of decaying solutions of the plane problem of the theory of elasticity for a semistrip. *Journal of Applied Mathematics and Mechanics*, 29(4):892–901, 1965.

K. Ha. Finite element analysis of sandwich plates: an overview. *Computers & Structures*, 37(4):397–403, 1990.

N. J. Hoff. Bending and buckling of rectangular sandwich plates. Technical report, Polytechnic Institute of Brooklyn, 1950.

C. Horgan. Saint-venant end effects for sandwich structures. In *Fourth International Conference on Sanwich Construction*, volume 1, pages 191–200. EMAS Publishing UK, 1998.

A. T. Jones. Exact natural frequencies for cross-ply laminates. *Journal of Composite Materials*, 4(4):476–491, 1970.

J. Kaplunov and D. Markushevich. Plane vibrations and radiation of an elastic layer lying on a liquid half-space. *Wave Motion*, 17(3):199–211, 1993.

J. Kaplunov and E. Nolde. Long-wave vibrations of a nearly incompressible isotropic plate with fixed faces. *The Quarterly Journal of Mechanics and Applied Mathematics*, 55(3):345–356, 2002.

J. Kaplunov, L. Y. Kossovich, and G. Rogerson. Direct asymptotic integration of the equations of transversely isotropic elasticity for a plate near cut-off frequencies. *Quarterly Journal of Mechanics and Applied Mathematics*, 53(2):323–341, 2000a.

J. Kaplunov, E. Nolde, and G. Rogerson. A low-frequency model for dynamic motion in pre-stressed incompressible elastic structures. *Proceedings of the Royal Society of London. Series A: Mathematical, Physical and Engineering Sciences*, 456(2003): 2589–2610, 2000b.

J. Kaplunov, E. Nolde, and G. Rogerson. An asymptotically consistent model for long-wave high-frequency motion in a pre-stressed elastic plate. *Mathematics and Mechanics of Solids*, 7(6):581–606, 2002a.

J. Kaplunov, E. Nolde, and G. Rogerson. Short wave motion in a pre-stressed incompressible elastic plate. *IMA Journal of Applied Mathematics*, 67(4):383–399, 2002b.

J. Kaplunov, G. Rogerson, and P. Tovstik. Localized vibration in elastic structures with slowly varying thickness. *The Quarterly Journal of Mechanics and Applied*

Mathematics, 58(4):645–664, 2005.

J. Kaplunov, E. Nolde, and G. A. Rogerson. An asymptotic analysis of initial-value problems for thin elastic plates. *Proceedings of the Royal Society A: Mathematical, Physical and Engineering Sciences*, 462(2073):2541–2561, 2006.

J. Kaplunov, D. Prikazchikov, and O. Sergushova. Multi-parametric analysis of the lowest natural frequencies of strongly inhomogeneous elastic rods. *Journal of Sound and Vibration*, 366:264–276, 2016.

J. Kaplunov, D. Prikazchikov, and L. Prikazchikova. Dispersion of elastic waves in a strongly inhomogeneous three-layered plate. *International Journal of Solids and Structures*, 113:169–179, 2017a.

J. Kaplunov, D. Prikazchikov, and L. Prikazchikova. Dispersion of elastic waves in laminated glass. *Procedia Engineering*, 199:1489–1494, 2017b.

J. Kaplunov, D. Prikazchikov, and L. Sultanova. Justification and refinement of Winkler–Fuss hypothesis. *Zeitschrift für angewandte Mathematik und Physik*, 69 (3):80, 2018.

J. Kaplunov, D. Prikazchikov, L. Prikazchikova, A. Nikonov, and T. Savšek. Multi-parametric dynamic analysis of lightweight elastic laminates. In *IOP Conference*

Series: Materials Science and Engineering, volume 683, page 012014. IOP Publishing, 2019a.

J. Kaplunov, D. Prikazchikov, L. Prikazchikova, and O. Sergushova. The lowest vibration spectra of multi-component structures with contrast material properties. *Journal of Sound and Vibration*, 445:132–147, 2019b.

J. Kaplunov, D. Prikazchikov, and L. Sultanova. Elastic contact of a stiff thin layer and a half-space. *Zeitschrift für angewandte Mathematik und Physik*, 70(1):22, 2019c.

J. Kaplunov, L. Prikazchikova, and M. Alkinidri. Antiplane shear of an asymmetric sandwich plate. *Continuum Mechanics and Thermodynamics*, pages 1–16, 2021.

J. D. Kaplunov, L. Y. Kossovitch, and E. Nolde. *Dynamics of thin walled elastic bodies*. Academic Press, 1998.

J.-S. Kim and S.-K. Chung. A study on the low-velocity impact response of laminates for composite railway bodyshells. *Composite Structures*, 77(4):484–492, 2007.

I. Kreja. A literature review on computational models for laminated composite and sandwich panels. *Open Engineering*, 2011.

I. I. Kudish, E. Pashkovski, S. S. Volkov, A. S. Vasiliev, and S. M. Aizikovich. Heavily loaded line ehl contacts with thin adsorbed soft layers. *Mathematics and Mechanics of Solids*, 25(4):1011–1037, 2020.

I. I. Kudish, S. S. Volkov, A. S. Vasiliev, and S. M. Aizikovich. Characterization of the behavior of different contacts with double coating. *Mathematics and Mechanics of Complex Systems*, 9:179–202, 2021. doi: 10.2140/memocs.2021.9.179.

S. Kulkarni and N. Pagano. Dynamic characteristics of composite laminates. *Journal of Sound and Vibration*, 23(1):127–143, 1972.

H. Lamb. On waves in an elastic plate. *Proceedings of the Royal Society of London. Series A, Containing papers of a mathematical and physical character*, 93(648): 114–128, 1917.

M. Lashhab, G. Rogerson, and L. Prikazchikova. Small amplitude waves in a pre-stressed compressible elastic layer with one fixed and one free face. *Zeitschrift für angewandte Mathematik und Physik*, 66(5):2741–2757, 2015.

K. C. Le. *Vibrations of shells and rods.* Springer Science & Business Media, 2012.

P. Lee and N. Chang. Harmonic waves in elastic sandwich plates. *Journal of Elasticity*, 9(1):51–69, 1979.

S. Leungvichcharoen and A. C. Wijeyewickrema. Dispersion effects of extensional waves in pre-stressed imperfectly bonded incompressible elastic layered composites. *Wave Motion*, 38(4):311–325, 2003.

L. Liu and K. Bhattacharya. Wave propagation in a sandwich structure. *International Journal of Solids and Structures*, 46(17):3290–3300, 2009.

A. E. H. Love. *A treatise on the mathematical theory of elasticity.* Cambridge university press, 2013.

M. Lutianov and G. A. Rogerson. Long wave motion in layered elastic media. *International Journal of Engineering Science*, 48(12):1856–1871, 2010.

T. P. Martin, C. N. Layman, K. M. Moore, and G. J. Orris. Elastic shells with high-contrast material properties as acoustic metamaterial components. *Physical Review B*, 85(16):161103, 2012.

G. I. Mikhasev and H. Altenbvach. *Thin-walled Laminated Structures.* Springer, 2019.

R. Mindlin. Flexural vibrations of elastic sandwich plates. Technical report, Department of Civil Engineering and Engineering Mechanics. Columbia University, 1959.

R. Mindlin. Waves and vibrations in isotropic, elastic plates. In *Proc Symposium on Naval Structural Mechanics*, pages 199–232. Pergamon Press, 1960.

R. Mines, C. Worrall, and A. Gibson. Low velocity perforation behaviour of polymer composite sandwich panels. *International Journal of Impact Engineering*, 21(10): 855–879, 1998.

K. Naumenko and V. A. Eremeyev. A layer-wise theory for laminated glass and photovoltaic panels. *Composite Structures*, 112:283–291, 2014.

T.-K. Nguyen, K. Sab, and G. Bonnet. First-order shear deformation plate models for functionally graded materials. *Composite Structures*, 83(1):25–36, 2008.

E. Nolde. Qualitative analysis of initial-value problems for a thin elastic strip. *IMA Journal of Applied Mathematics*, 72(3):348–375, 2007.

E. Nolde and G. Rogerson. Long wave asymptotic integration of the governing equations for a pre-stressed incompressible elastic layer with fixed faces. *Wave Motion*, 36(3):287–304, 2002.

E. Nolde, L. Prikazchikova, and G. Rogerson. Dispersion of small amplitude waves in a pre-stressed, compressible elastic plate. *Journal of Elasticity*, 75(1):1–29, 2004.

E. Nolde, A. Pichugin, and J. Kaplunov. An asymptotic higher-order theory for rectangular beams. *Proceedings of the Royal Society A: Mathematical, Physical and Engineering Sciences*, 474(2214):20180001, 2018.

A. K. Noor, W. S. Burton, and C. W. Bert. Computational models for sandwich panels and shells. *Applied Mechanics Reviews*, 49(3):155, 1996.

A. V. Pichugin and G. A. Rogerson. A two-dimensional model for extensional motion of a pre-stressed incompressible elastic layer near cut-off frequencies. *IMA Journal of Applied Mathematics*, 66(4):357–385, 2001.

A. V. Pichugin and G. A. Rogerson. An asymptotic membrane-like theory for long-wave motion in a pre-stressed elastic plate. *Proceedings of the Royal Society of London. Series A: Mathematical, Physical and Engineering Sciences*, 458(2022): 1447–1468, 2002a.

A. V. Pichugin and G. A. Rogerson. Anti-symmetric motion of a pre-stressed incompressible elastic layer near shear resonance. *Journal of Engineering Mathematics*, 42(2):181–202, 2002b.

B. Popescu and D. H. Hodges. On asymptotically correct Timoshenko-like anisotropic beam theory. *International Journal of Solids and Structures*, 37(3):535–558, 2000.

L. Prikazchikova, Y. Ece Aydın, B. Erbaş, and J. Kaplunov. Asymptotic analysis of an anti-plane dynamic problem for a three-layered strongly inhomogeneous laminate. *Mathematics and Mechanics of Solids*, 25(1):3–16, 2020.

M. S. Qatu. *Vibration of laminated shells and plates.* Elsevier, 2004.

J. N. Reddy. *Mechanics of laminated composite plates and shells: theory and analysis.* CRC press, 2003.

E. L. Reiss and S. Locke. On the theory of plane stress. *Quarterly of Applied Mathematics*, 19(3):195–203, 1961.

E. Reissner. On bending of elastic plates. *Quarterly of Applied Mathematics*, 5(1): 55–68, 1947.

E. Reissner. On the derivation of the theory of thin elastic shells. *Journal of Mathematics and Physics*, 42(1-4):263–277, 1963.

J. M. Renno. *Dynamics and control of membrane mirrors for adaptive optic applications.* PhD thesis, Virginia Tech, 2008.

J. Rion. Ultra-light photovoltaic composite sandwich structures. Technical report, EPFL, 2008.

G. Rogerson and K. Sandiford. On small amplitude vibrations of pre-stressed laminates. *International Journal of Engineering Science*, 34(8):853–872, 1996.

G. Rogerson and K. Sandiford. Flexual waves in incompressible pre-stressed elastic composites. *The Quarterly Journal of Mechanics and Applied Mathematics*, 50(4): 597–624, 1997.

G. Rogerson, I. Kirillova, and Y. A. Parfenova. Boundary layers near the reflected and transmitted dilatational wave fronts in a composite cylindrical shell. In *Theories of Plates and Shells*, pages 193–200. Springer, 2004.

G. A. Rogerson, K. J. Sandiford, and L. A. Prikazchikova. Abnormal long wave dispersion phenomena in a slightly compressible elastic plate with non-classical boundary conditions. *International Journal of Non-Linear Mechanics*, 42(2):298–309, 2007.

M. Y. Ryazantseva and F. K. Antonov. Harmonic running waves in sandwich plates. *International Journal of Engineering Science*, 59:184–192, 2012.

S. V. Sorokin. Analysis of wave propagation in sandwich plates with and without heavy fluid loading. *Journal of Sound and Vibration*, 271(3-5):1039–1062, 2004.

A. Spencer. *Continuum Mechanics*. Longman Scientific & Technical, Harlow, UK, 1988.

N. Stephen. Considerations on second order beam theories. *International Journal of Solids and Structures*, 17(3):325–333, 1981.

N. Stephen. The second spectrum of Timoshenko beam theory - further assessment. *Journal of Sound and Vibration*, 292(1-2):372–389, 2006.

O. J. Tassicker. *Aspects of forces on charged particles in electrostatic precipitators.* PhD thesis, Department of Electrical Engineering Wollongong University Colledge, 1972.

I. Tolstoy and E. Usdin. Wave propagation in elastic plates: low and high mode dispersion. *The Journal of the Acoustical Society of America*, 29(1):37–42, 1957.

L. Torre and J. Kenny. Impact testing and simulation of composite sandwich structures for civil transportation. *Composite Structures*, 50(3):257–267, 2000.

P. Tovstik. Free high-frequency vibrations of anisotropic plates of variable thickness. *Journal of Applied Mathematics and Mechanics*, 56(3):390–395, 1992.

P. Tovstik and T. Tovstik. Generalized TimoshenkoReissner models for beams and plates, strongly heterogeneous in the thickness direction. *ZAMM-Journal of Applied Mathematics and Mechanics/Zeitschrift für Angewandte Mathematik und Mechanik*, 2017.

M. Van Dyke. Perturbation methods in fluid mechanics/Annotated edition. *NASA STI/Recon Technical Report A*, 75:46926, 1975.

J. R. Vinson. *The behavior of sandwich structures of isotropic and composite materials.* CRC Press, 1999.

K. Viverge, C. Boutin, and F. Sallet. Model of highly contrasted plates versus experiments on laminated glass. *International Journal of Solids and Structures*, 102: 238–258, 2016.

C. Y. Wang and C. Wang. *Structural vibration: exact solutions for strings, membranes, beams, and plates.* CRC Press, 2016.

Y.-Y. Yu. Forced flexural vibrations of sandwich plates in plane strain. *Journal of Applied Mechanics*, 27(3):535, 1960.

D. Zenkert. *An introduction to sandwich construction.* Engineering Materials Advisory Services, 1995.

A. Zinno, E. Fusco, A. Prota, and G. Manfredi. Multiscale approach for the design of composite sandwich structures for train application. *Composite Structures*, 92 (9):2208–2219, 2010.